nature medicine

SUPPLEMENTARY INFORMATION

https://doi.org/10.1038/s41591-020-0841-4

In the format provided by the authors and unedited.

Development and validation of serological markers for detecting recent *Plasmodium vivax* infection

Rhea J. Longley[1,2,3,21], Michael T. White[4,21], Eizo Takashima[5], Jessica Brewster[1], Masayuki Morita[5], Matthias Harbers[6,7], Thomas Obadia[4,8], Leanne J. Robinson[1,2,9], Fumie Matsuura[6], Zoe S. J. Liu[1,2], Connie S. N. Li-Wai-Suen[1,2], Wai-Hong Tham[2,10], Julie Healer[2,10], Christele Huon[11], Chetan E. Chitnis[11], Wang Nguitragool[12], Wuelton Monteiro[13,14], Carla Proietti[15,16], Denise L. Doolan[15,16], Andre M. Siqueira[17], Xavier C. Ding[18], Iveth J. Gonzalez[18], James Kazura[19], Marcus Lacerda[13,20], Jetsumon Sattabongkot[3], Takafumi Tsuboi[5] and Ivo Mueller[1,2,4] ✉

[1]Population Health and Immunity Division, Walter and Eliza Hall Institute of Medical Research, Melbourne, Victoria, Australia. [2]Department of Medical Biology, University of Melbourne, Melbourne, Victoria, Australia. [3]Mahidol Vivax Research Unit, Faculty of Tropical Medicine, Mahidol University, Bangkok, Thailand. [4]Unité Malaria: Parasites et Hôtes, Département Parasites et Insectes Vecteurs, Institut Pasteur, Paris, France. [5]Division of Malaria Research, Proteo-Science Center, Ehime University, Matsuyama, Japan. [6]CellFree Sciences Co., Ltd., Yokohama, Japan. [7]RIKEN Center for Integrated Medical Sciences (IMS), Yokohama, Japan. [8]Hub de Bioinformatique et Biostatistique, Département Biologie Computationnelle, Institut Pasteur, USR 3756 CNRS, Paris, France. [9]Burnet Institute, Melbourne, Victoria, Australia. [10]Infection and Immunity Division, Walter and Eliza Hall Institute of Medical Research, Melbourne, Victoria, Australia. [11]Malaria Parasite Biology and Vaccines, Department of Parasites & Insect Vectors, Institut Pasteur, Paris, France. [12]Department of Molecular Tropical Medicine and Genetics, Faculty of Tropical Medicine, Mahidol University, Bangkok, Thailand. [13]Fundacão de Medicina Tropical Dr. Heitor Vieira Dourado, Manaus, Brazil. [14]Universidade do Estado do Amazonas, Manaus, Brazil. [15]Centre for Molecular Therapeutics, Australian Institute of Tropical Health and Medicine, James Cook University, Cairns, Queensland, Australia. [16]QIMR Berghofer Medical Research Institute, Brisbane, Queensland, Australia. [17]Instituto Nacional de Infectologia Evandro Chagas–Fiocruz, Rio de Janeiro, Brazil. [18]Foundation for Innovative New Diagnostics, Geneva, Switzerland. [19]Center for Global Health and Diseases, Case Western Reserve University, Cleveland, OH, USA. [20]Instituto Leônidas & Maria Deane (Fiocruz), Manaus, Brazil. [21]These authors contributed equally: Rhea J. Longley, Michael T. White. ✉e-mail: mueller@wehi.edu.au

Development and validation of serological markers for detecting recent exposure to *Plasmodium vivax* infection

Rhea J Longley*, Michael T White*, Eizo Takashima, Jessica Brewster, Masayuki Morita, Matthias Harbers, Thomas Obadia, Leanne J Robinson, Fumie Matsuura, Shih-Jung (Zoe) Liu, Connie S. N. Li Wai Suen, Wai-Hong Tham, Julie Healer, Christele Huon, Chetan E. Chitnis, Wang Ngruitragool, Wuelton Monteiro, Carla Proietti, Denise L. Doolan, Xavier C. Ding, Iveth J. Gonzalez, James Kazura, Marcus Lacerda, Jetsumon Sattabongkot, Takafumi Tsuboi, Ivo Mueller

* Joint first authors. Technical queries to Michael White (michael.white@pasteur.fr).

Supplementary Methods and Results

1. Antigen discovery phase

1.1. Linear model for decay of antibody response

The half-lives of the antibody responses to the 307 *P. vivax* proteins in the antigen discovery phase were estimated using previously described methods (Longley 2017). Estimated half-lives were calculated for an additional 35 proteins for this manuscript. In brief, 32 Thai individuals and 33 Brazilian individuals were followed longitudinally after a clinical episode of *P. vivax*. These individuals were treated with primaquine to prevent relapses, and the absence of any blood-stage *Plasmodium* parasites during follow-up was confirmed by testing blood samples by PCR. Antibody responses were measured at 0, 3, 6 and 9 months using the AlphaScreen assay. Denote A_{ijk} to be the antibody titre in participant i to protein j at time t_k which can be described by the following linear model:

$$\log\left(A_{ijk}\right) \sim \left(\log\left(\alpha_j^0\right) + \log\left(\alpha_{ij}\right)\right) + \left(r_j^0 + r_{ij}\right)t_k + \varepsilon_j \qquad \text{(S1)}$$

where α_j^0 is the geometric mean titre (GMT) at the time of infection; $\log(\alpha_{ij})$ is a random effect accounting for the difference between participant i's initial antibody titre and the population-level GMT; r_j^0 is the average rate of decay of antibodies to protein j in the population; r_{ij} is a random effect for the difference between the decay rate of individual i with the population-level average; and $\varepsilon_j \sim N(0, \sigma_{m,j})$ is a Normally distributed error term. In particular we assume that the random effects for the initial antibody titres are Normally distributed: $\log(\alpha_{ij}) \sim N(0, \sigma_{A,j})$, and that the random effects for the variation in decay rates are also Normally distributed: $r_{ij} \sim N(0, \sigma_{r,j})$.

The model was only fitted to individuals who were seropositive at baseline. This model also generated an estimate of the total variation in the data (arising from initial antibody level measured, the rate of antibody decay and the measurement error). Table S1 provides the estimated antibody half-lives and relevant parameters for all 342 proteins (see separate excel file).

1.2. Estimation of time since infection using antibodies to a single *P. vivax* protein

The linear regression model for the decay of antibody titres described in equation (S1) has three sources of variation: (i) variation in initial antibody response following infection; (ii) between individual variation in antibody decay rate; and (iii) measurement error. Notably, all these sources of variations are described by Normal distributions (Figure S1a) so their combined variation will also be described by a Normal distribution. Therefore, $x_{ij} = \log(A_{ij})$, the expected log antibody titre in individual i to protein j at time t, can be described by the following distribution:

$$x_{ij} \sim N\left(\alpha_j^0 + r_j t, \sigma_{\alpha,j}^2 + t^2\sigma_{r,j}^2 + \sigma_{m.j}^2\right) \qquad \text{(S2)}$$

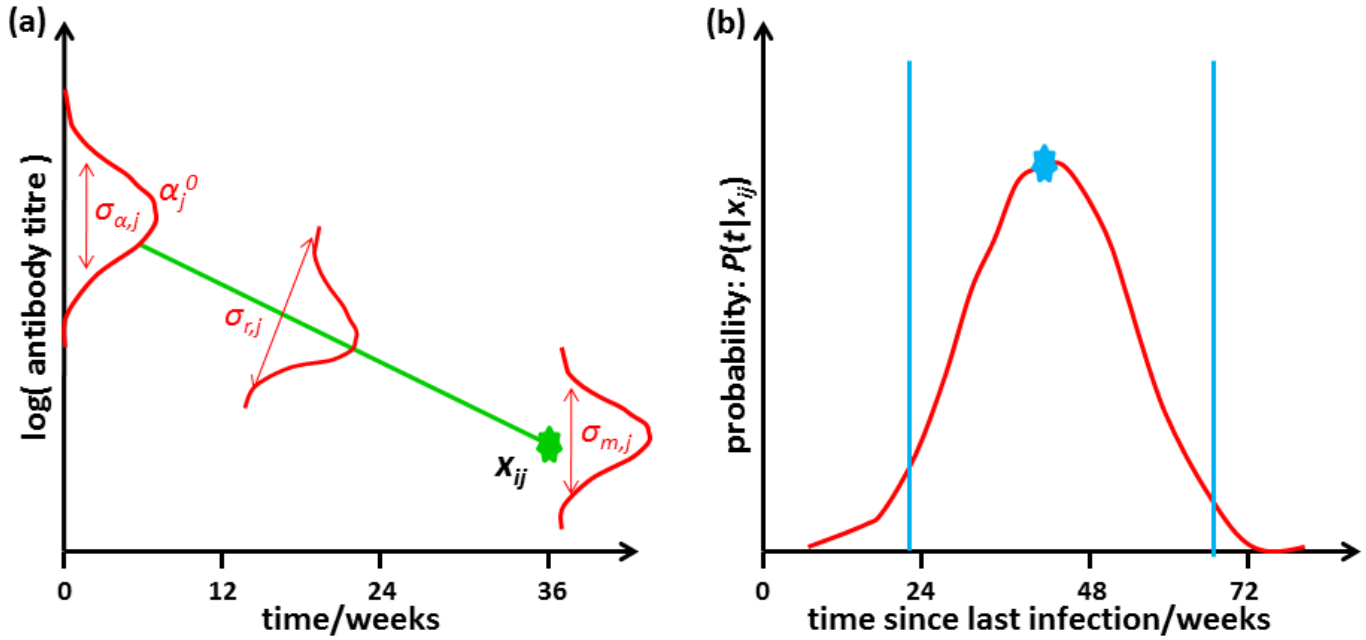

Figure S1: Association between measured antibody titre and time since infection. **(a)** There are three sources of variation in the log antibody titre x_{ij} measured at time t since last infection: (i) variation in initial antibody titre; (ii) between individual variation in antibody decay rate; and (iii) measurement error. **(b)** Given estimates of the sources of variation, we can estimate the distribution of the time since last infection. The maximum likelihood estimate and the 95% confidence intervals of our estimate are indicated in blue.

The probability distribution of the expected antibody titre in individual i to protein j at time t is given by the following distribution:

$$\mathbf{P}\left(x_{ij}\middle|t\right)=\frac{1}{\sqrt{2\pi\left(\sigma_{\alpha,j}^2+t^2\sigma_{r,j}^2+\sigma_{m,j}^2\right)}}e^{-\frac{\left(x_{ij}-\alpha_j^0-r_j^0t\right)^2}{2\left(\sigma_{\alpha,j}^2+t^2\sigma_{r,j}^2+\sigma_{m,j}^2\right)}} \qquad \text{(S3)}$$

Note that we have $x_{ij} \in (-\infty, +\infty)$, as x_{ij} denotes the log antibody titre and measurements of antibody titre are assumed to be positive. The probability distribution for the time since infection t given measured antibody titre x_{ij} can be calculated by inverting equation (S3) using Bayes rule (see also Borremans 2016).

$$\mathbf{P}\left(t\middle|x_{ij}\right)=\frac{\mathbf{P}\left(x_{ij}\middle|t\right)\mathbf{P}\left(t\right)}{\mathbf{P}\left(x_{ij}\right)} \qquad \text{(S4)}$$

The time since last infection will have a lower bound of zero. We can choose to impose an upper bound of either the individual's age a or positive infinity. Choosing positive infinity allows us to better handle the case where an individual was never infected – the low measured antibody titres will be consistent with a very large time since last infection, possibly greater than the age of the individual. Therefore we should only restrict t to the interval $(0, a)$ if we know for certain that the individual has been infected. In practice, we choose some large time t_{max} = 100 years for our upper bound. We assume $\boldsymbol{P}(\ t\ )$ denotes a uniform distribution on the interval $(0, t_{max})$. $\boldsymbol{P}(\ x_{ij}\ )$ is a normalising constant which is calculated via numerical integration to ensure that $\boldsymbol{P}(\ t \mid x_{ij}\ )$ denotes a probability distribution.

Equation (S4) provides a probability distribution for the time since last infection. For the purposes of a diagnostic test we may be more interested in obtaining a binary classification, e.g. was the individual infected within the last 9 months? We denote z_i to be an indicator variable denoting whether individual i was infected within the last 9 months ($z_i = 1$) or not ($z_i = 0$). The probabilities of these two events can be calculated as follows:

$$\begin{aligned}\mathbf{P}\left(z_i=1\middle|x_{ij}\right)&=\int_0^9\mathbf{P}\left(t\middle|x_{ij}\right)dt\\ \mathbf{P}\left(z_i=0\middle|x_{ij}\right)&=\int_9^{t_{\max}}\mathbf{P}\left(t\middle|x_{ij}\right)dt\end{aligned} \qquad \text{(S5)}$$

1.3. Estimation of time since infection using antibodies to multiple *P. vivax* proteins

The methods above describe how measurements of antibody responses to a single protein can be used to estimate the time since last infection. However, in practice there is too much noise to make an accurate estimate of time since last infection with a single protein. Increasing the number of measured antibodies can increase the information content in our data allowing us to obtain more accurate estimates of time since last infection. In particular, selecting antibodies with a range of half-lives may increase our power to resolve infection times more accurately.

Figure S2 shows a schematic of the kinetics of antibodies to two proteins. We have rapidly decaying antibody 1 and slowly decaying antibody 2. At baseline, antibody titres are likely to be correlated, so we assume that initial titre following infection is described by a multivariate Normal distribution with covariance matrix Σ_α. The between individual rates of antibody decay may also be correlated (i.e. all antibody titres may decay particularly quickly in some individuals) so we also assume that decay rates are described by a multivariate Normal distribution with covariance matrix Σ_r. Finally, there will be measurement error associated with each antibody. In particular, we assume the measurement errors between different antibodies are independent so that the total measurement error can be described by a multivariate Normal distribution with diagonal covariance matrix Σ_m. For the case with measurements of antibodies to J proteins, we have:

$$\mathbf{P}\left(x_i \middle| t\right) = \left(2\pi\right)^{-\frac{J}{2}} \left|\Sigma_\alpha + t^2\Sigma_r + \Sigma_m\right|^{-\frac{1}{2}} e^{-\frac{1}{2}\left(x_i-\alpha^0-r^0t\right)^T\left(\Sigma_\alpha+t^2\Sigma_r+\Sigma_m\right)^{-1}\left(x_i-\alpha^0-r^0t\right)} \qquad \text{(S6)}$$

The time since last infection can be estimated given the multivariate probability distribution for the measured vector of antibody titres x_i and the classification probability for the 9 month threshold can be estimated as follows:

$$\begin{aligned}\mathbf{P}\left(z_i = 1 \middle| x_i\right) &= \int_0^9 \mathbf{P}\left(t \middle| x_i\right) dt \\ \mathbf{P}\left(z_i = 0 \middle| x_i\right) &= \int_9^{t_{\max}} \mathbf{P}\left(t \middle| x_i\right) dt\end{aligned} \qquad \text{(S7)}$$

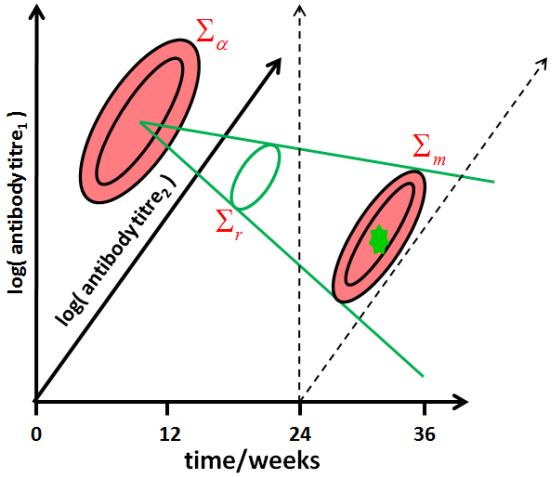

Figure S2: Kinetics of multiple antibodies. The variance in initial antibody titre, antibody decay rates and measurement error are now described by covariance matrices which account for the correlations between antibodies.

1.4. Identifying optimal combinations of *P. vivax* proteins using simulated annealing

Machine learning algorithms take data from a large number of streams and identify which data streams have the most signal for classifying output. Such methods typically involve a greedy algorithm that will provide a good but not necessarily optimal solution. Greedy algorithms take the next best step, i.e. including the next protein that gives the biggest increase in predictive power. As such they may provide a locally optimal solution but not necessarily a globally optimal solution. Simulated annealing algorithms provide an alternative to greedy algorithms that usually provide a higher likelihood of obtaining a globally optimal solution (Kirkpatrick 1983).

Here we describe how a simulated annealing algorithm can be applied to the method for estimating time since infection described above, to select combinations of proteins that maximise the likelihood of correctly classifying infections within the last 9 months. Assume that J measurements of antibodies are available. We want to select some subset of these that maximises predictive power. Denote y to be a vector of 0's and 1's indicating whether the j^{th} antibody is included in our panel. Thus for example with $J = 9$ we may have

$$y = \left(0,0,1,1,0,1,0,0,1\right) \qquad \text{(S8)}$$

The vector of binary states depicted in equation (S8) will correspond to a vector of antibody measurements from individual *i* as follows:

$$x_i = \left(x_{i,3}, x_{i,4}, x_{i,6}, x_{i,9} \right) \quad \text{(S9)}$$

Let z_i be an indicator denoting whether individual *i* was infected in the last 9 months ($z_i = 1$) or not ($z_i = 0$). Given data from *I* individuals on measured antibody responses, we can calculate the probability that the individual was infected within the last 9 months $\boldsymbol{P}$ ($z_i = 1 \mid x_i$) or greater than 9 months ago $\boldsymbol{P}$ ($z_i = 0 \mid x_i$). We can then write down the likelihood of the data as follows:

$$L(y) = \prod_{i=1}^{I} \mathbf{P}\left(z_i = 1 \middle| x_i \right)^{z_i} \mathbf{P}\left(z_i = 0 \middle| x_i \right)^{1-z_i} \quad \text{(S10)}$$

The challenge is to select a binary vector *y* corresponding to a combination of proteins that maximises the likelihood in equation (S10) and thus has the highest likelihood of correctly classifying infections according to whether they occurred in the last 9 months.

If we have *J* proteins, there are 2^J combinations of proteins. For $J > 15$ it is not computationally feasible to test all possible combinations. We therefore utilise a simulated annealing algorithm for exploring the state space of combinations and identifying the optimal combinations subject to various constraints (e.g. enforcing a maximum of $J_{max} = 10$ proteins to a panel).

Here we describe a simulated annealing algorithm with *M* iterations and an exponential cooling schedule such that the temperature at iteration $m \leq M$ is $T_m = e^{-\left(\frac{M-m}{M}\right)}$. It is also assumed that $J_{\max}$ is the maximum number of proteins that can be considered in a panel.

- At iteration *m* we have binary state vector y_m with likelihood $L(y_m)$.
- Generate new binary state vector y_{m+1} by switching two randomly selected binary states.
- Reject the new state if $\sum_{j=1}^{J} y_{j,m+1} > J_{\max}$
- Accept the new state with probability $\min\left(1, e^{-\left(\frac{L(y_m)-L(y_{m+1})}{T_{m+1}}\right)} \right)$

The algorithm was repeated 100 times with different starting points and $M = 30000$ iterations. This resulted in 100 possibly different estimates of optimal combinations of proteins.

1.5. Additional results

The output of the search of the space of protein combinations is summarised in Figure 2E of the main manuscript. Additional properties of the 104 *P. vivax* proteins considered in the second round of the antigen discovery phase are shown in Figure S3.

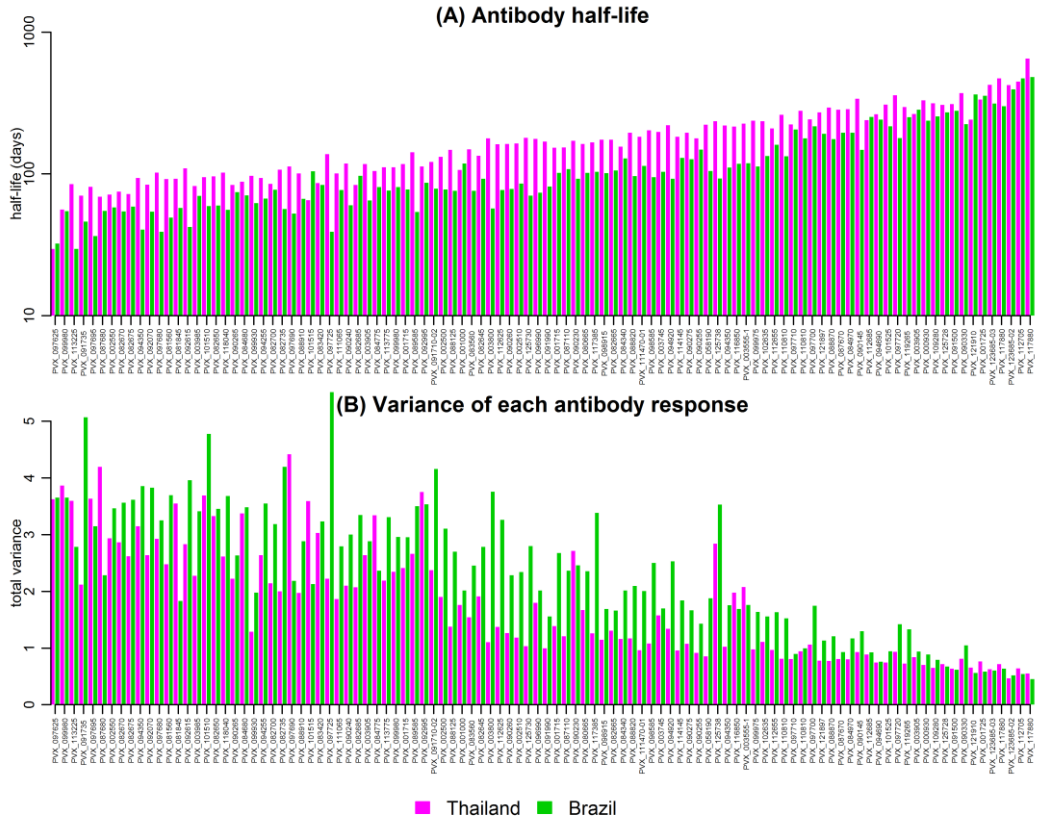

Figure S3: Estimates of (A) antibody half-life, and (B) the variance of each antibody response for 104 *P. vivax* proteins in the antigen discovery phase.

A property of the simulated annealing based search strategy applied to this data set is that, on average, the most predictive proteins are selected first, much like what would be expected for a greedy algorithm. This leads to a phenomenon of diminishing returns, where the addition of each new protein causes sequentially smaller improvements in likelihood and classification performance (Figure S4).

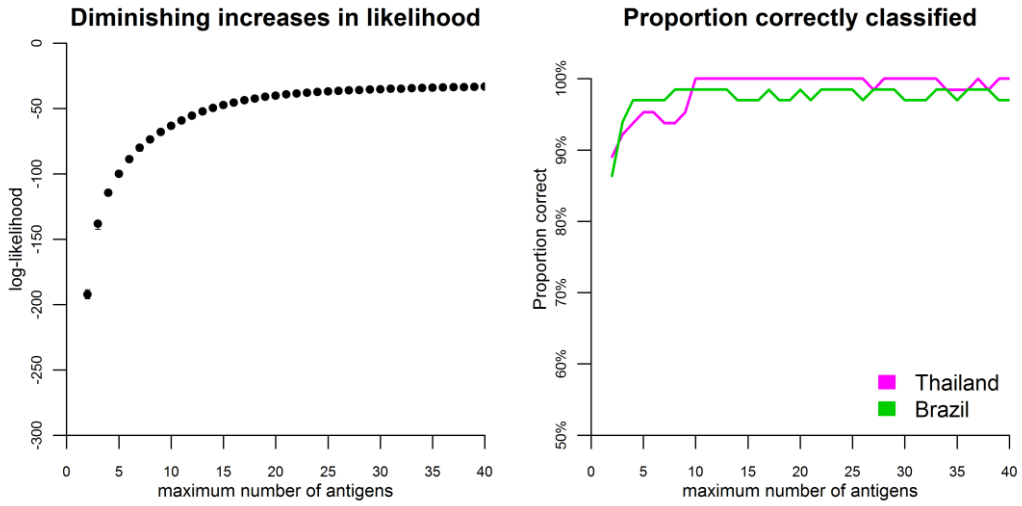

Figure S4: Increasing the maximum number of proteins allowed in a panel leads to diminishing increases in likelihood and classification performance. Note that classification performance was assessed using the same training and testing data set, i.e. without cross-validation.

2. Validation phase

2.1. Supplementary data on all proteins

Table S2 shows the association of antibody level with current *P. vivax* infections (see separate excel file). Extended Data Figure 2 shows the distribution of measured antibody responses to the 60 proteins used in the validation phase in the Thai, Brazilian, Solomon Islands and negative control cohorts, as well as the association with time since last PCR-detected blood-stage *P. vivax* infection.

2.2. Targets for classification

The data in Extended Data Figure 2 demonstrate that for many proteins, there is a clear relationship between measured antibody response and time since last blood-stage *P. vivax* infection. Data from several proteins may be combined to optimise classification performance, however, first it is necessary to provide a definition of what we are attempting to classify and how optimal performance is selected.

Why 9 months? In theory it is possible to provide quantitative estimates of the time since last infection, however a more useful outcome in practice is whether an individual has been infected within some past time period. Throughout this analysis, we have investigated the potential for measurements of antibody response from a sample to identify whether the sampled individual had a PCR-detected blood-stage *P. vivax* infection within the last 9 months. This time period was selected because:

(i) In the geographic regions studied, relapses are expected to occur at a frequency of every 1 – 2 months, with hypnozoites remaining in the liver for up to 1 – 2 years (Battle 2014, White 2016). Although some individuals are expected to be infected with liver-stage hypnozoites for greater than 1 year, the highest incidence of relapses is anticipated to occur within the first 9 months following mosquito bite infection (White 2011). Therefore, an individual with blood-stage *P. vivax* parasites detected by PCR within the last 9 months is expected to be a likely hypnozoite carrier.
(ii) When specifying a threshold for time since last infection, it is optimal if this threshold falls within a region where we have data. This allows us to have observed infections both before and after the threshold. The three longitudinal cohorts studied had follow-up for 12 months, thus 9 months falls within this window.

What classification performance are we targeting? An ideal diagnostic tool would achieve 100% sensitivity (where all infected individuals are correctly identified as infected) and 100% specificity (where all non-infected individuals are correctly identified as non-infected). In reality there is a trade-off between sensitivity and specificity, which can be characterised by a Receiver Operating Characteristic (ROC) curve. The particular balance between sensitivity and specificity will be selected according to the public health needs of the proposed diagnostic tool. Here we define three target product profiles (TPP) based on sensitivity-specificity trade-off (Ding 2017).

(i) Medium-sensitivity & medium-specificity (e.g. sens = 80% & spec = 80%). This target assigns equal weight to sensitivity and specificity. This target can be optimised by maximising the area under the ROC curve (AUC).
(ii) High-sensitivity & low-specificity (e.g. sens = 95% & spec = 50%). This target would be useful if one wishes to identify and treat all likely hypnozoite carriers, but some degree of over-treatment is acceptable.
(iii) Low-sensitivity & high-specificity (e.g. sens = 50% & spec = 95%). This target would be appropriate in surveillance settings for verifying the absence of transmission, where false-positives would incorrectly indicate ongoing transmission. The issue of false-negatives can be overcome by increasing survey size.

2.3. Initial search of protein combinations

Here we investigate how combinations of the 60 proteins in Extended Data Figure 2 were used to identify individuals with blood-stage *P. vivax* parasites detected by PCR within the last 9 months. A linear discriminant analysis (LDA) classification algorithm was used for this search strategy. There were 1,770 ways of choosing two out of 60 proteins, 34,220 ways of choosing three proteins, 487,635 ways of choosing four proteins, and 5,461,512 ways of choosing five proteins. All combinations up to size four were exhaustively evaluated to optimise classification performance for the three target product profiles (TPP) defined in section 2.2.

To investigate combinations of size five, we identified the 100 best combinations of four proteins for each of the three TPPs. We added all possible remaining proteins to each of these 300 combinations, and then assessed the classification performance of all of these combinations of size five. A similar procedure was implemented to investigate classification performance of combinations of proteins up to size eight. Figure S5 shows an overview of classification performance.

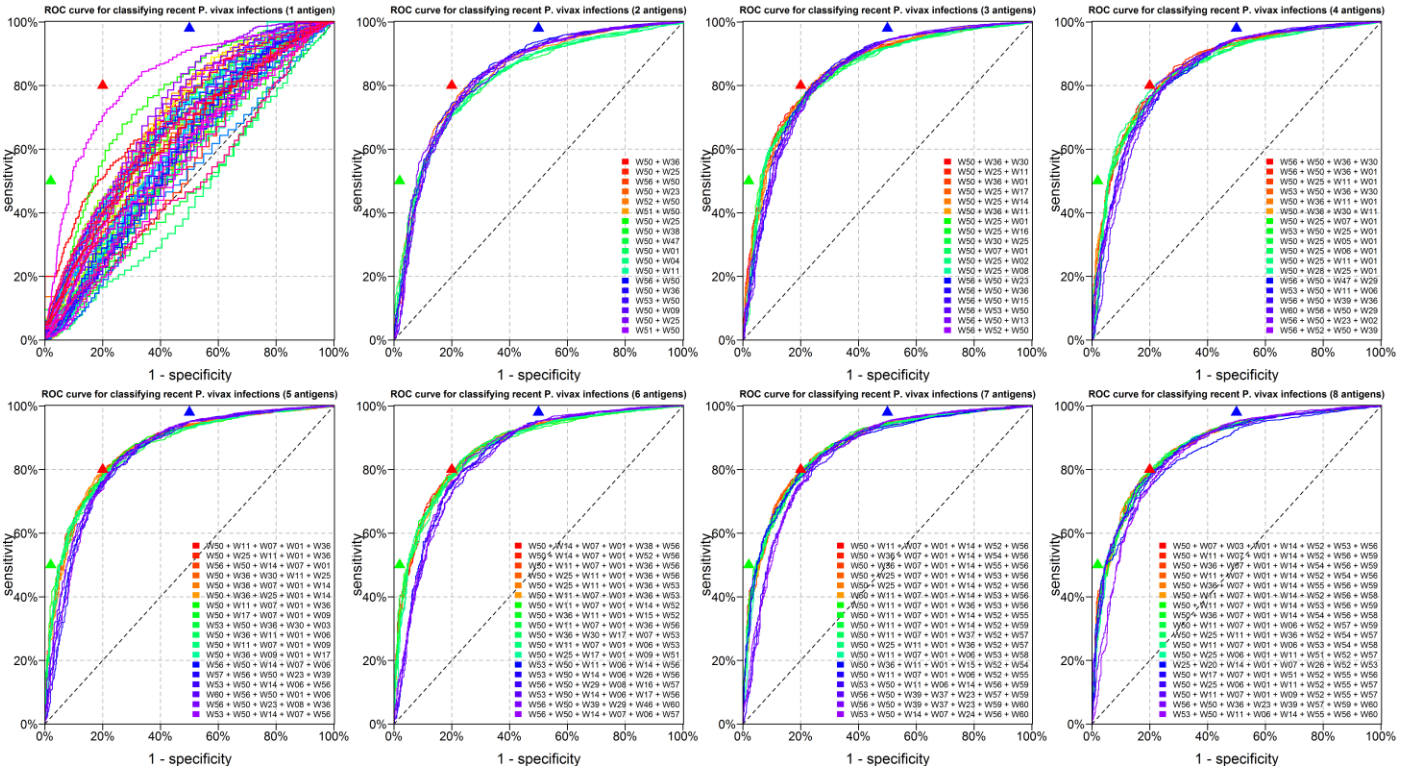

Figure S5: Performance of LDA classifier for combinations of proteins up to size eight for identifying individuals with blood-stage *P. vivax* infection within the last 9 months. The same training and testing data sets were used: data from endemic cohorts in Thailand, Brazil and the Solomon Islands plus negative control cohorts. The three triangles represent the TPPs in section 2.2. The red triangle is the medium-sensitivity & medium-specificity target, the blue triangle is the high-sensitivity & low-specificity target, and the green triangle is the low-sensitivity & high specificity target.

A network diagram was used to visualise which combinations of proteins provided the best classification performance (Figure S6). This network was generated based on the calculated AUC from ROC curves generated by an LDA classifier applied to all combinations of 4 from 60 proteins.

Denote c_n where $1 \leq n \leq N = 487{,}635$ to be a combination of four proteins, and let AUC_n be the area under the ROC curve generated by linear discriminant analysis. First re-order n so that AUC_n is decreasing. We now calculate a vector of vertex weights V_j for each protein, and a matrix of edge weights M_{jk} for connections between proteins. The vertex weights are proportional to how frequently a protein is selected in combinations with high ranking AUC.

$$V_j = \exp\left(-C_V \sum_{n=1}^{N} \mathbf{1}\left(j \in c_n \right) n \right) \qquad \text{(S11)}$$

The edge weights are proportional to how frequently pairs of proteins are selected in combinations with high ranking AUC.

$$M_{jk} = \exp\left(-C_M \sum_{n=1}^{N} \mathbf{1}\left(j \in c_n \right) \mathbf{1}\left(k \in c_n \right) n \right) \qquad \text{(S12)}$$

C_V and C_M are scaling constants manually selected to ensure good network visualisations. The network corresponding to the matrix M_{jk} was plotted using the igraph R package with a Fruchterman-Reingold network layout. The sizes of the plotted vertices were scaled using V_j. The generated network of antigen combinations is shown in Figure S6.

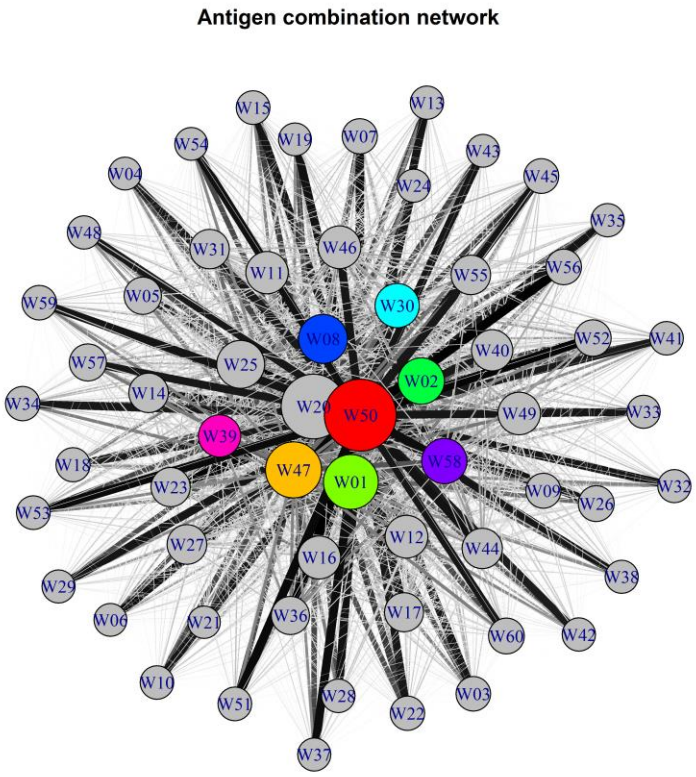

Figure S6: Network visualization of antigens selected in combinations of size 4. Larger vertices denote antigens frequently selected in combinations that maximise area under the curve (AUC) for classification. W20 was not selected because it was a construct of the same protein as W50 (PVX_094255).

The coloured proteins at the central vertices of the network in Figure S6 represent the antigens that perform best at classification in combinations of size 4. Notably, there is a very high degree of concordance between these antigens and those with the highest AUC when used for single antigen classification in Table S2.

Extended Data Figure 3 presents an additional analysis demonstrating one of the key factors of the determinant of AUC, namely background reactivity measured in negative controls. In particular, lower mean relative antibody units in the negative control panels were associated with greater AUC. Figure S7 presents the results of a sensitivity analysis to determine how much the inclusion of data from negative control panels affects classification performance, compared to just using data from the longitudinal cohorts in endemic regions. The removal of data from the negative control participants leads to a decrease in classification performance (i.e. the AUC decreases). This is expected as negative controls are very easy to correctly classify as negative, compared to individuals living in endemic regions, see Extended Data Figure 4 for a breakdown of classification accuracy by category. However, what is important is that the decrease in AUC is comparatively modest.

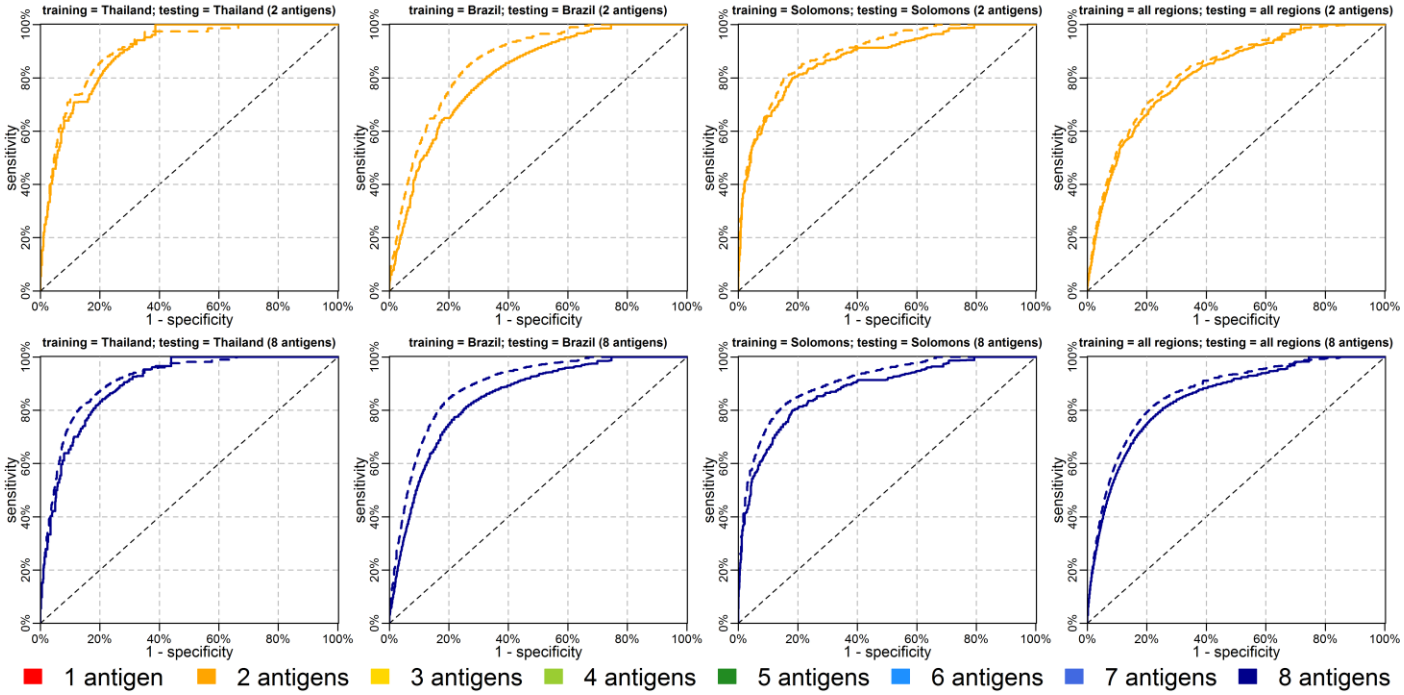

Figure S7: Assessment of the role of removing data from negative control participants on classification performance using a Random Forests classifier. Dashed lines denote predictions with negative control participants included, and solid lines denote predictions with negative control participants excluded.

Extended Data Figure 4 provides a more detailed breakdown of the classification performance of the composite algorithm with an 80% sensitivity and 80% specificity target. Note that for this target, the best performing component algorithm was Random Forests. The results demonstrate that the algorithm has very good performance at correctly classifying negative controls as not exposed. The poorest classification performance was in individuals infected 9 – 12 months ago, many of whom were incorrectly classified as having had infection within the last 9 months.

2.4. Classification algorithms

Let X_{ij} denote the matrix of measured log antibody titres in individual i to protein j. Let z_i denote whether individual i was infected in the last 9 months ($z_i = 1$) or not ($z_i = 0$). The classification performance of algorithms is assessed through cross-validation whereby 2/3 of individuals are randomly selected to be in a training data set ($X_{ij,\text{train}}$ and $z_{i,\text{train}}$), and the remaining 1/3 selected in the testing data set ($X_{ij,\text{test}}$ and $z_{i,\text{test}}$). This process is repeated 1000 times.

2.4.1. Statistical classifiers

A number of conventional classifiers from the fields of statistical inference and machine learning were repeatedly applied to the training and testing data sets. Classifiers considered were:

(i) logistic regression
(ii) LDA
(iii) quadratic discriminant analysis (QDA)
(iv) decision trees
(v) random forests

These classifiers are widely used and are described in detail by Hastie, Tibshirani & Friedman. All algorithms were implemented in R. Decision trees were implemented using the rpart R package. Random forests were implemented using the randomForest R package.

The random forests algorithm can also be used to generate a variable importance plot which can provide a ranking of antigens in terms of their contribution to classification performance (Figure S8).

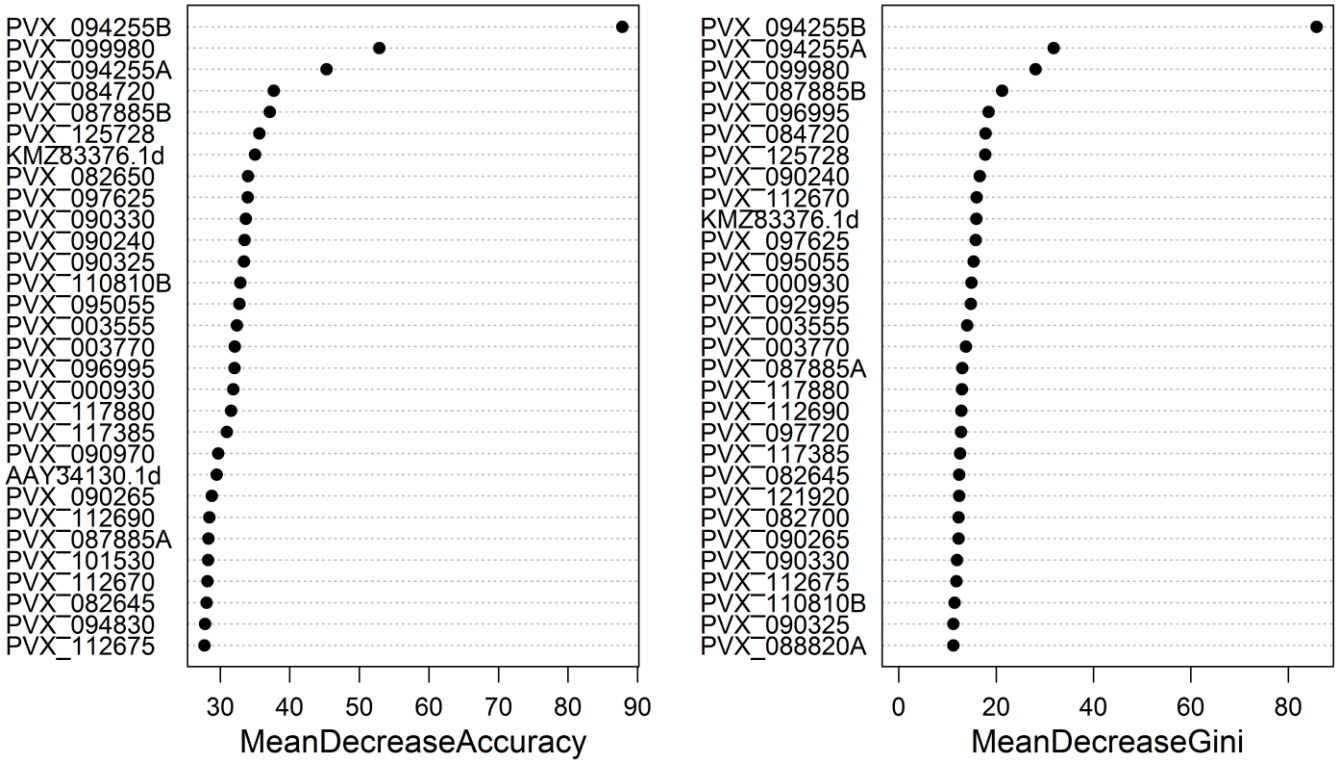

Figure S8: Variable importance plot for identifying antigens that contribute to optimal classification in a random forests algorithm generated using the varImpPlot function from the randomForest R package. Note the high degree of concordance between the listed proteins and those in the network in Figure S6.

2.4.2. Antibody kinetics classifiers

Section 2.4.1 lists the 'off-the-shelf' statistical classifiers. Here we describe how information on antibody kinetics can be incorporated into a classification algorithm.

Antibody kinetics algorithm #1

This is similar to the LDA and QDA algorithms. Let $\alpha_{\text{train,0-9m}}$ and $\Sigma_{\text{train,0-9m}}$ be the mean and covariance matrix of the multi-variate normal distribution fitted to data from recently infected individuals in the training data. Let $\alpha_{\text{train,9m+}}$ and $\Sigma_{\text{train,9m+}}$ be the mean and covariance matrix of the multi-variate normal distribution fitted to data from individuals without recent infection in the training data. For a measurement of antibody responses from an individual in the testing data set $x_{i,\text{test}}$ we can calculate the relative probabilities as follows:

$$\begin{aligned} Q\left(z_{i,\text{test}}=0\middle|x_{i,\text{test}}\right) &= \frac{1}{\sqrt{2\pi\left|\Sigma_{\text{train,9m+}}\right|}} e^{-\frac{1}{2}\left(\left(x_{i,\text{test}}-\alpha_{\text{train,9m+}}\right)^T \Sigma_{\text{train,9m+}}^{-1}\left(x_{i,\text{test}}-\alpha_{\text{train,9m+}}\right)\right)} \\ Q\left(z_{i,\text{test}}=1\middle|x_{i,\text{test}}\right) &= \frac{1}{\sqrt{2\pi\left|\Sigma_{\text{train,0-9m}}\right|}} e^{-\frac{1}{2}\left(\left(x_{i,\text{test}}-\alpha_{\text{train,0-9m}}\right)^T \Sigma_{\text{train,0-9m}}^{-1}\left(x_{i,\text{test}}-\alpha_{\text{train,0-9m}}\right)\right)} \end{aligned} \quad \text{(S13)}$$

These probabilities can be normalised as follows:

$$\begin{aligned} P\left(z_{i,\text{test}}=0\middle|x_{i,\text{test}}\right) &= \frac{Q\left(z_{i,\text{test}}=0\middle|x_{i,\text{test}}\right)}{Q\left(z_{i,\text{test}}=0\middle|x_{i,\text{test}}\right)+Q\left(z_{i,\text{test}}=1\middle|x_{i,\text{test}}\right)} \\ P\left(z_{i,\text{test}}=1\middle|x_{i,\text{test}}\right) &= \frac{Q\left(z_{i,\text{test}}=1\middle|x_{i,\text{test}}\right)}{Q\left(z_{i,\text{test}}=0\middle|x_{i,\text{test}}\right)+Q\left(z_{i,\text{test}}=1\middle|x_{i,\text{test}}\right)} \end{aligned} \quad \text{(S14)}$$

Antibody kinetics algorithm #2

This algorithm extends antibody kinetics algorithm #1 by accounting for the data available in the known time since last infection in the training data set $T_{i,\text{train}}$. The first step is to use a linear regression model on those individuals with a detected blood-stage infection to estimate the geometric mean antibody titre at the time of last PCR-detectable blood-stage infection and the decay rate of antibodies over time:

$$X_{ij,\text{train}} \sim \log\left(\alpha_j^0\right) + r_j^0 T_{i,\text{train}} + \varepsilon_j \quad \text{(S15)}$$

where $X_{ij,\text{train}}$ is the log antibody titer to protein j from individual i in the training data set, $T_{i,\text{train}}$ is the time since last PCR-detected blood-stage infection in individual i in the training data set, r_j^0 is the estimated antibody decay rate, $\log(\alpha_j^0)$ is the intercept term, i.e. the log of the geometric mean titre at the time of infection, and ε_j is Normally distributed measurement error. Note that in contrast to equation (S1), the serological data utilised here are from a cross-sectional and not a longitudinal survey, therefore the resulting regression model does not account for mixed effects.

We can now follow the approach outlined above in Section 1.3.

$$\begin{aligned} \mathbf{P}\left(x_i\middle|t, z_i=0\right) &= \left(2\pi\right)^{-\frac{J}{2}}\left|\Sigma_{\text{train,9m+}}+t^2\Sigma_r\right|^{-\frac{1}{2}} e^{-\frac{1}{2}\left(x_i-\alpha^0-r^0t\right)^T\left(\Sigma_{\text{train,9m+}}+t^2\Sigma_r\right)^{-1}\left(x_i-\alpha^0-r^0t\right)} \\ \mathbf{P}\left(x_i\middle|t, z_i=1\right) &= \left(2\pi\right)^{-\frac{J}{2}}\left|\Sigma_{\text{train,0-9m}}+t^2\Sigma_r\right|^{-\frac{1}{2}} e^{-\frac{1}{2}\left(x_i-\alpha^0-r^0t\right)^T\left(\Sigma_{\text{train,0-9m}}+t^2\Sigma_r\right)^{-1}\left(x_i-\alpha^0-r^0t\right)} \end{aligned} \quad \text{(S16)}$$

And these can be inverted similar to above to give

$$\begin{aligned} \mathbf{P}\left(z_i=1\middle|x_i\right) &= \int_0^9 \mathbf{P}\left(x_i\middle|t, z_i=1\right)dt \\ \mathbf{P}\left(z_i=0\middle|x_i\right) &= \int_9^{t_{\max}} \mathbf{P}\left(x_i\middle|t, z_i=0\right)dt \end{aligned} \quad \text{(S17)}$$

2.4.3. Assessment of the role of age and *P. falciparum* infection

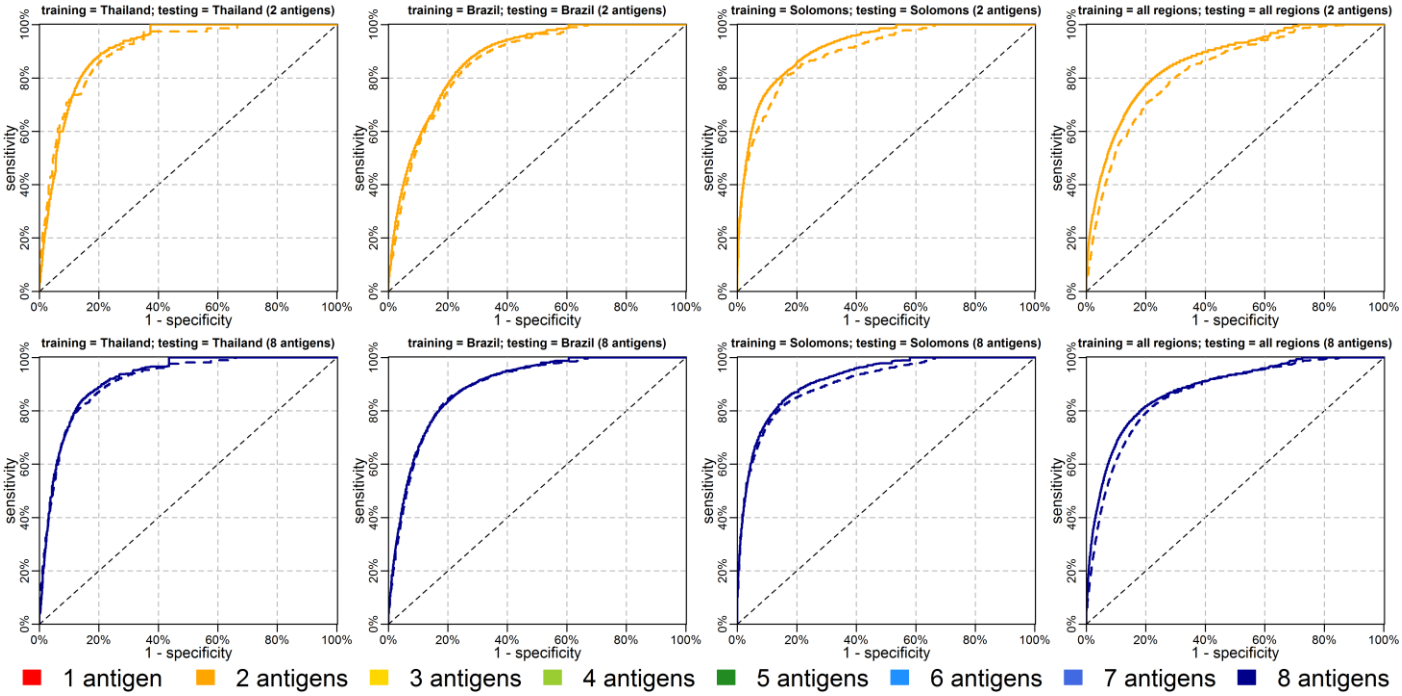

Figure S9: Assessment of incorporating information on an individual's age into a Random Forests classifier. Age was incorporated as a continuous variable in years. The Random Forests classifier was selected for this sensitivity analysis because of the flexibility with which it could incorporate information on age. Dashed lines denote predictions without age, and solid lines denote predictions with age.

Figure S9 demonstrates that once a sufficient number of antibody responses are accounted for in the classification algorithm, there is no incremental benefit to also incorporating age. The information provided by an individual's age is correlated with their antibody levels: on average older people have higher antibody levels. When age is included in a classifier with a single antigen, it acts to normalise an individual's lifetime exposure. When the number of measured antibody responses is increased, this information required for normalization is instead be obtained from the antibody levels themselves.

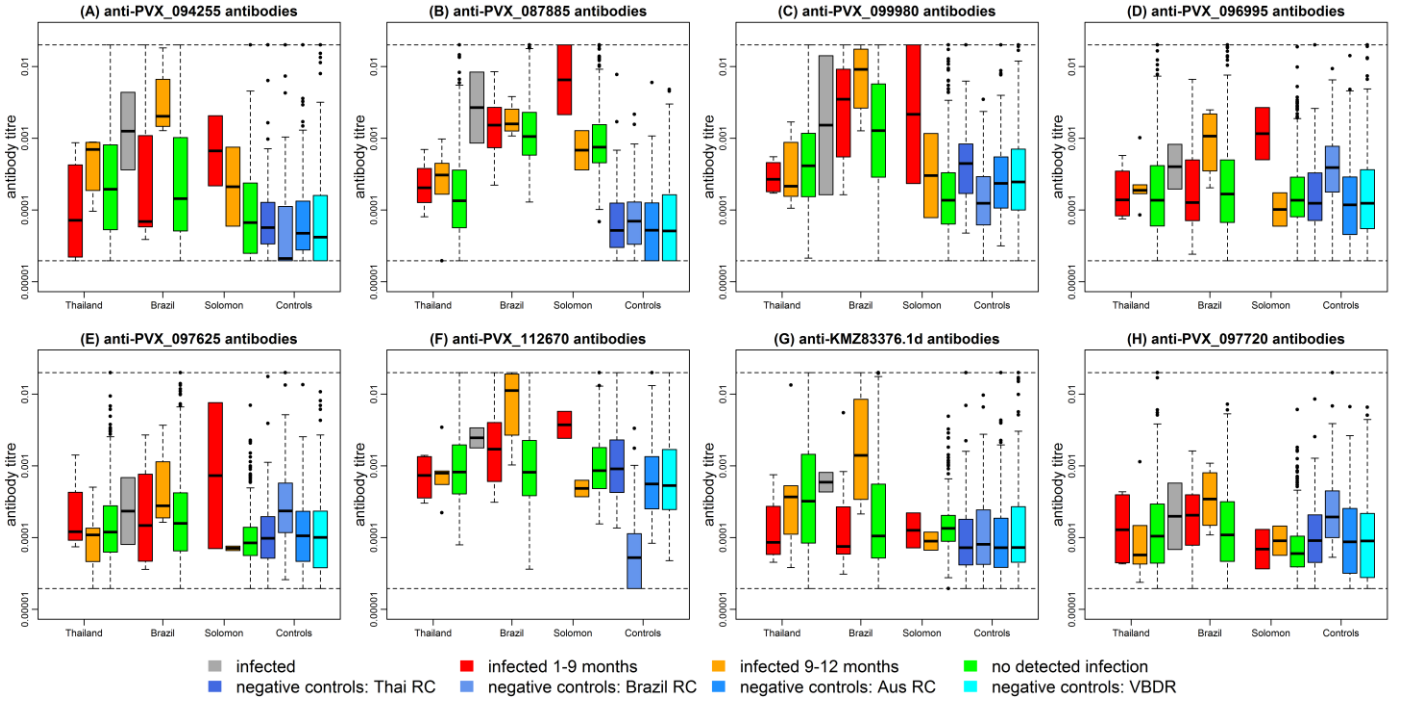

Figure S10: Association between measurements of our top eight *P. vivax* proteins and time since last PCR detected blood-stage *P. falciparum* infection. Note that individuals with any sample PCR positive for *P. vivax* have been removed. For all eight proteins in each of the three cohorts, there was no significant difference in relative antibody units between individuals with no PCR-detected blood-stage *P. falciparum* and individuals with a blood-stage *P. falciparum* in the last 9 months (two-sided Student's t-test).

2.5. Cross-validated classification performance

Figure S11 shows a comparison of the cross-validated classification performance of the seven algorithms described above on several data sets. All algorithms provide comparable performance, indicating that they all capture the same signal in the data. For the combination of eight proteins, the Random Forests algorithm performs the best on average. The antibody kinetics algorithm 2 performs best at hitting high specificity targets. These seven algorithms can be designated as components of a composite classification algorithm. For a desired target of sensitivity and specificity, the composite classification algorithm outputs the results of the best performing component algorithm. Note that this approach is conceptually similar to the SuperLearner algorithm used in Helb 2015.

The same concept can be applied to combinations of proteins. For example, there are 28 ways to choose a combination of two proteins from eight proteins. Thus we can generate 28 ROC curves and choose the one that performs best for a given target of sensitivity and specificity.

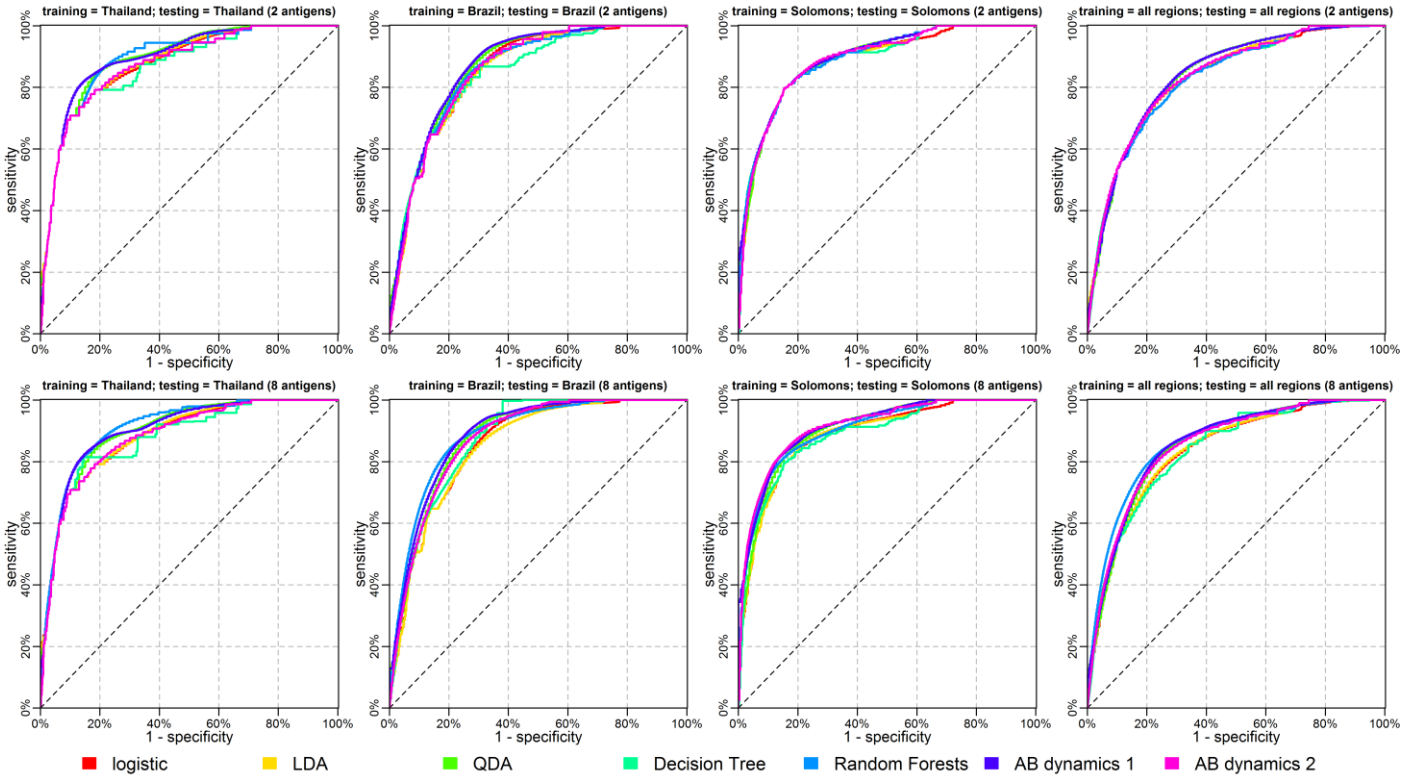

Figure S11: Receiver operating characteristic (ROC) curves depicting comparison of cross-validated classification performance for the seven classification algorithms considered. For a given sensitivity and specificity target, the composite classification algorithm selects the best of the seven component algorithms. Its ROC curve can be considered as the convex hull of the ROC curves for the seven component algorithms. All curves presented are the median of 1000 repeat cross-validations.

In Extended Data Figure 5 we see that the composite classification algorithm has comparable performance across a wide range of training and testing data sets. For example, when trained on Brazilian data, the classifier performs well on Thai data. This repeated pattern suggests that an algorithm trained in one epidemiological setting can be applied to other epidemiological settings.

3. Pilot Application phase – supplementary results

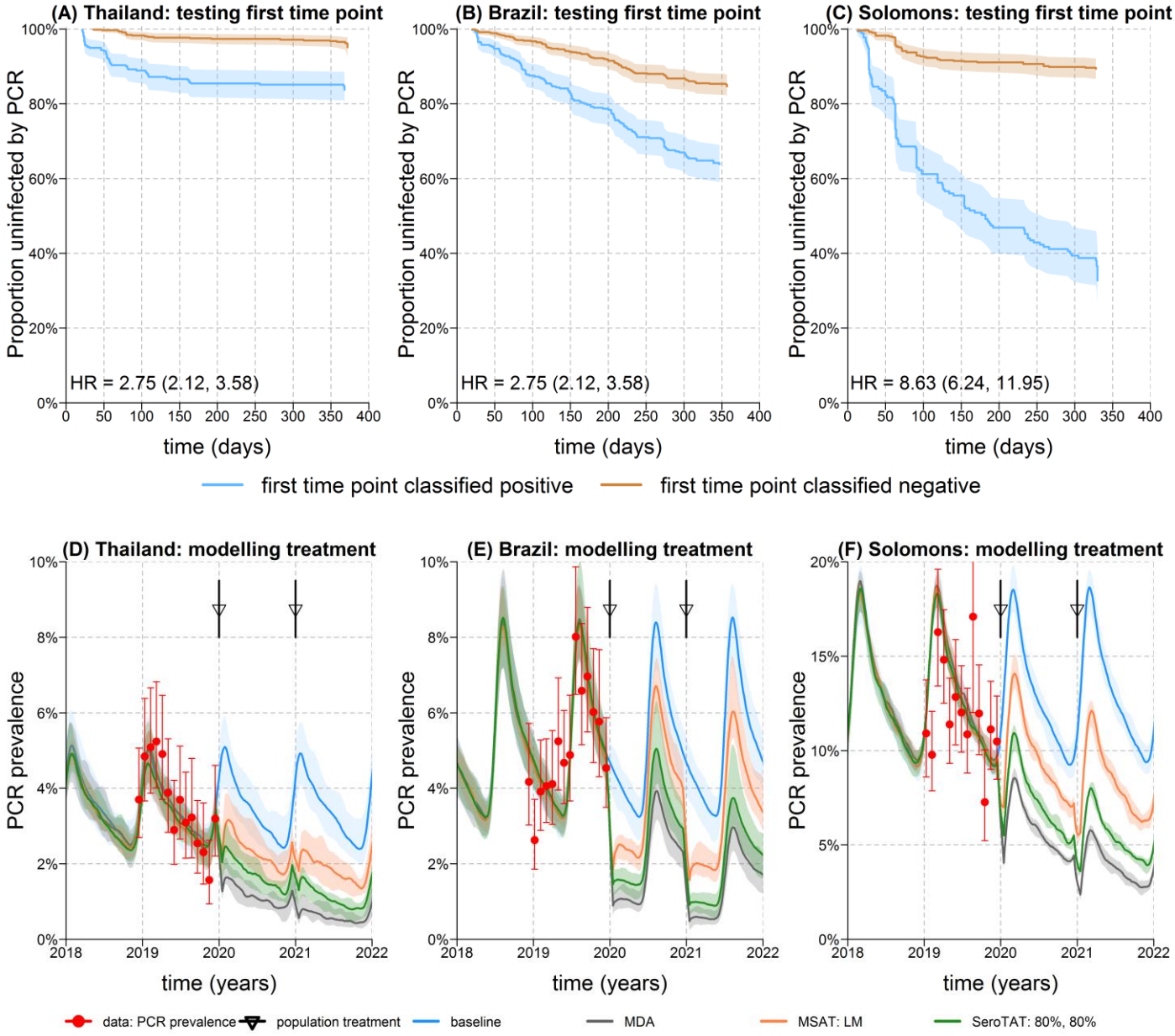

Figure S12: Pilot application phase. (A-C) Kaplan-Meier analyses of time to first *P. vivax* blood-stage infection detected by PCR. Individuals who were *P. vivax* PCR positive at the start of follow-up have been excluded. Using measured antibody responses at the first time point, participants were classified as positive (blood-stage infection within the past 9 months) or negative. Hazards ratio (HR) were calculated using Cox proportional hazards, and were statistically significant with $P < 10^{-10}$ in all cases. (D-F) Prediction from a mathematical model of *P. vivax* transmission of the effect of population-level treatment strategies with primaquine at 80% coverage. The model was calibrated to longitudinal data on PCR prevalence, and the potential impact of two rounds of treatment in 2020 and 2021 were simulated. The percentage reduction in transmission was calculated as the estimated prevalence in June 2021 compared to June 2019.

References

1. Borremans B, Hens N, Beutels P, Leirs H, Reijniers J. Estimating time of infection using prior serological and individual information can greatly improve incidence estimation of human and wildlife infections. *PLOS Comp Biol* 2016; **12**(5): e1004882
2. Longley RJ, White MT, Takashima E, Morita M, Kanoi BN, Li Wai Suen CSN, et al. Naturally acquired antibody responses to more than 300 *Plasmodium vivax* proteins in three geographic regions. *PLOS Negl Trop Dis* 2017; **11**(9): e0005888
3. Kirkpatrick S, Gelatt Jr CD, Vecchi MP. Optimization by simulated annealing. *Science* 1983; **220**(4598): 671-680
4. Battle KE, Karhunen MS, Bhatt S, Gething PW, Howes RE, *et al*. Geographical variation in *Plasmodium vivax* relapse. *Malar J* 2014; **13**(144)
5. White MT, Shirreff G, Karl S, Ghani AC, Mueller I. Variation in relapse frequency and the transmission potential of *Plasmodium vivax* malaria. *Proc Roy Soc B* 2016; **283**(1827)
6. White N. Determinants of relapse periodicity in *Plasmodium vivax* malaria. *Malar J* 2011; **10**(297)
7. Ding X, Paz Ade M, Baird JK, Cheng Q, Cunningham J, *et al.* Defining the next generation of *Plasmodium vivax* diagnostic tests for control and elimination: Target product profiles. *PLoS Neg Trop Dis* 2017; **11**(4): e0005516
8. Hastie T, Tibshirani R, Friedman J. The elements of statistical learning: Data mining, inference and prediction. Second Edition. *Springer-Verlag* 2009
9. Helb DA, Tetteh KA, Felgner PL, Skinner J, Hubbard A, Arinaitwe E, et al. Novel serologic biomarkers provide accurate estimates of recent *Plasmodium falciparum* exposure for indviduals and communities. *PNAS* 2015; **112**(32): E4438-4447

Table S1. Estimated antibody half-lives from antigen discovery phase.

Protein	Thai_r_mean	Thai_r_mean_low	Thai_r_mean_high	Thai_d_half	Thai_d_half_low	Thai_d_half_high	Braz_r_mean	Braz_r_mean_low	Braz_r_mean_high	Braz_d_half	Braz_d_half_low	Braz_d_half_high
PVX_092275	-0.0012	-0.0027	3.00E-04	565	254	Inf	-0.0012	-0.0028	4.00E-04	583	248	Inf
PVX_089345	-0.0033	-0.006	-5.00E-04	213	115	1384	-0.0025	-0.0051	0	276	137	Inf
PVX_000995	-0.0107	-0.0142	-0.0071	65	49	97	-0.0095	-0.0151	-0.0038	73	46	180
PVX_113225	-0.0043	-0.006	-0.0025	163	115	277	-0.0095	-0.0146	-0.0044	73	48	157
PVX_110970	-0.0154	-0.0209	-0.0098	45	33	70	-0.0097	-0.0149	-0.0045	71	46	155
PVX_099670	-0.0084	-0.0123	-0.0046	82	57	151	-0.0022	-0.0051	7.00E-04	313	136	Inf
PVX_091500	-0.0023	-0.0031	-0.0014	306	224	485	-0.0027	-0.0041	-0.0013	257	171	518
PVX_080225	-0.0101	-0.0145	-0.0058	68	48	120	-0.0012	-0.0039	0.0014	562	178	Inf
PVX_115355	-0.0175	-0.025	-0.0099	40	28	70	-0.0044	-0.0079	-9.00E-04	158	88	777
PVX_111470-01	-0.0016	-0.0024	-9.00E-04	425	294	771	-0.0024	-0.0037	-0.0011	289	190	612
PVX_086150	-0.001	-0.0015	-4.00E-04	713	451	1710	-0.002	-0.0029	-0.0011	346	236	649
PVX_090255	-0.0021	-0.0032	-9.00E-04	338	218	749	-0.0064	-0.0106	-0.0023	108	65	305
PVX_113775	-0.005	-0.0087	-0.0014	138	80	489	-0.0187	-0.0272	-0.0102	37	26	68
PVX_099035	-0.0076	-0.0109	-0.0044	91	64	158	-0.0053	-0.0105	0	132	66	802254
PVX_097700	-0.0031	-0.0053	-8.00E-04	226	131	825	-0.0065	-0.0105	-0.0025	107	66	279
PVX_083420	-0.0061	-0.0097	-0.0026	113	71	270	-0.0085	-0.0145	-0.0024	82	48	285
PVX_082680	-0.0096	-0.0145	-0.0048	72	48	146	-0.0074	-0.0131	-0.0017	94	53	420
PVX_090945	-0.0042	-0.0069	-0.0014	166	100	488	-7.00E-04	-0.0022	8.00E-04	948	308	Inf
PVX_099975	-0.0103	-0.0148	-0.0058	67	47	119	-0.0057	-0.011	-4.00E-04	122	63	1654
PVX_112705	-0.0015	-0.0023	-8.00E-04	448	308	820	-0.0016	-0.0027	-6.00E-04	422	255	1230
PVX_091435	-0.0021	-0.0043	2.00E-04	332	160	Inf	-8.00E-04	-0.0021	5.00E-04	843	327	Inf
PVX_085445-1	-0.0046	-0.0078	-0.0015	149	89	463	-0.0011	-0.0029	7.00E-04	612	235	Inf
PVX_087110	-0.0045	-0.0063	-0.0027	154	110	253	-0.0068	-0.0115	-0.002	102	60	339
PVX_003905	-0.0135	-0.0183	-0.0086	52	38	80	-0.0067	-0.0133	-1.00E-04	104	52	11108
PVX_123685-02	-0.0016	-0.0022	-0.0011	424	316	642	-0.0019	-0.003	-9.00E-04	362	235	794
PVX_000975	-0.0087	-0.0127	-0.0047	80	55	148	-0.0033	-0.0076	0.001	212	92	Inf
PVX_090215	-0.011	-0.0151	-0.0069	63	46	101	-0.0073	-0.012	-0.0026	95	58	269

PVX_084720	-0.0073	-0.0106	-0.0041	95	66	170	-0.0093	-0.0144	-0.0043	74	48	162
PVX_092275	-0.0012	-0.0027	3.00E-04	565	254	Inf	-0.0012	-0.0028	4.00E-04	583	248	Inf
PVX_003800	-0.0083	-0.0113	-0.0052	84	61	132	-0.0134	-0.02	-0.0068	52	35	101
PVX_112655	-0.0035	-0.0058	-0.0012	197	119	583	-0.0072	-0.0107	-0.0037	96	65	186
PVX_096350	-0.0058	-0.0094	-0.0022	120	74	320	-0.0025	-0.0053	2.00E-04	273	130	Inf
PVX_088850	-0.0065	-0.0106	-0.0023	107	65	300	-0.0023	-0.0052	6.00E-04	301	134	Inf
PVX_085445	0.0022	-0.0021	0.0065	Inf	336	Inf	-0.0044	-0.0089	0	156	78	Inf
PVX_101590	-0.0052	-0.009	-0.0014	133	77	481	-0.0022	-0.0059	0.0016	318	117	Inf
PVX_116695	-0.01	-0.0139	-0.0061	70	50	114	-0.0062	-0.0109	-0.0014	113	63	502
PVX_112675	-0.0015	-0.0022	-7.00E-04	478	308	1062	-0.0029	-0.0041	-0.0017	240	169	413
PVX_101500	-0.0122	-0.016	-0.0084	57	43	83	-0.0079	-0.0145	-0.0014	88	48	505
PVX_092245	-0.0031	-0.0057	-6.00E-04	220	122	1147	-8.00E-04	-0.0019	4.00E-04	892	359	Inf
PVX_090145	-0.0031	-0.0042	-0.002	223	165	343	-0.0036	-0.0055	-0.0018	190	126	388
PVX_087140	-0.0088	-0.012	-0.0056	79	58	124	-0.0075	-0.0121	-0.003	92	57	233
PVX_118525	-0.0097	-0.0147	-0.0046	72	47	150	-0.0026	-0.0067	0.0015	266	103	Inf
PVX_094350	-0.0033	-0.0048	-0.0018	209	143	385	-0.0049	-0.0086	-0.0013	141	81	553
PVX_101485	-0.0057	-0.0087	-0.0027	122	80	257	-0.0021	-0.0045	3.00E-04	335	155	Inf
PVX_041190	-0.008	-0.0113	-0.0046	87	61	149	-0.0063	-0.0115	-0.001	111	60	723
PVX_083560	-0.0084	-0.0123	-0.0046	82	56	152	-0.0106	-0.0167	-0.0046	65	42	152
PVX_117005	-0.0101	-0.0145	-0.0058	68	48	119	-0.0077	-0.013	-0.0023	90	53	299
PVX_111470-02	-0.0075	-0.0114	-0.0035	93	61	196	-0.011	-0.0166	-0.0054	63	42	129
PVX_099980	-0.0072	-0.0089	-0.0054	97	78	128	-0.012	-0.0155	-0.0085	58	45	82
PVX_115045	-0.0144	-0.0195	-0.0093	48	36	75	-0.0179	-0.0253	-0.0105	39	27	66
PVX_114145	-0.0025	-0.0035	-0.0015	279	198	468	-0.0042	-0.0065	-0.002	164	107	351
PVX_096280	-0.013	-0.0178	-0.0082	53	39	85	-0.0033	-0.0071	5.00E-04	210	98	Inf
PVX_097710	-0.0077	-0.0119	-0.0035	90	58	198	-0.0053	-0.0104	-3.00E-04	130	66	2743
PVX_089330	-0.0041	-0.0069	-0.0013	170	100	548	-0.0016	-0.0038	6.00E-04	430	182	Inf
PVX_082675	-0.0039	-0.0051	-0.0026	180	135	269	-0.0108	-0.0169	-0.0047	64	41	146
PVX_094670	-0.0055	-0.0088	-0.0023	125	79	307	-0.0027	-0.0058	3.00E-04	256	120	Inf

PVX_099975	-0.0103	-0.0148	-0.0058	67	47	119	-0.0057	-0.011	-4.00E-04	122	63	1654
PVX_088810	-0.0124	-0.0169	-0.0078	56	41	88	-0.0059	-0.011	-8.00E-04	117	63	866
PVX_117385	-0.0042	-0.0061	-0.0022	167	113	319	-0.0076	-0.0142	-9.00E-04	92	49	797
PVX_085445-2	-0.0087	-0.0125	-0.0049	80	55	142	-6.00E-04	-0.0019	6.00E-04	1074	372	Inf
PVX_118445	-0.0082	-0.012	-0.0044	85	58	158	-0.0018	-0.004	5.00E-04	392	173	Inf
PVX_003905	-0.0135	-0.0183	-0.0086	52	38	80	-0.0067	-0.0133	-1.00E-04	104	52	11108
PVX_123685-03	-0.0021	-0.003	-0.0012	330	230	583	-0.0032	-0.0051	-0.0014	213	135	503
PVX_000975	-0.0087	-0.0127	-0.0047	80	55	148	-0.0033	-0.0076	0.001	212	92	Inf
PVX_085980	-0.0099	-0.0153	-0.0046	70	45	152	-0.0111	-0.0179	-0.0043	63	39	162
PVX_096070	-0.007	-0.0107	-0.0033	99	65	210	-0.0036	-0.0077	5.00E-04	195	90	Inf
PVX_092995	-0.0099	-0.0128	-0.007	70	54	99	-0.016	-0.0241	-0.008	43	29	87
PVX_099980	-0.0072	-0.0089	-0.0054	97	78	128	-0.012	-0.0155	-0.0085	58	45	82
PVX_003805	-0.0083	-0.0119	-0.0047	84	58	148	-0.0104	-0.0159	-0.005	66	44	140
PVX_112660	-0.0104	-0.0156	-0.0052	66	44	132	-0.0032	-0.0064	0	217	109	46520
PVX_092070	-0.0047	-0.0069	-0.0025	147	100	277	-0.0099	-0.0158	-0.0041	70	44	168
PVX_090260	-0.0082	-0.0114	-0.0049	85	61	142	-0.0094	-0.0153	-0.0034	74	45	201
PVX_084970	-0.003	-0.0058	-1.00E-04	235	120	4939	-0.0079	-0.0134	-0.0023	88	52	303
PVX_119355	-0.0067	-0.0097	-0.0036	104	72	191	-0.0065	-0.012	-0.0011	106	58	652
PVX_121945	-0.011	-0.0144	-0.0076	63	48	91	-0.0046	-0.0088	-3.00E-04	152	78	2449
PVX_080665	-0.0043	-0.0059	-0.0026	162	117	267	-0.0075	-0.0125	-0.0025	93	56	275
PVX_101530	-0.002	-0.0029	-0.0011	346	239	629	-0.0025	-0.0039	-0.0011	274	177	608
PVX_087680	-0.0047	-0.0067	-0.0026	149	103	271	-0.0098	-0.015	-0.0047	70	46	149
PVX_091735	-0.0042	-0.0064	-0.0021	164	108	335	-0.0089	-0.0141	-0.0037	78	49	185
PVX_097930	-0.0117	-0.0168	-0.0066	59	41	106	-0.009	-0.0167	-0.0013	77	41	553
PVX_121875	-0.0036	-0.0047	-0.0025	192	147	275	-0.0044	-0.0075	-0.0013	158	92	553
PVX_094350	-0.0033	-0.0048	-0.0018	209	143	385	-0.0049	-0.0086	-0.0013	141	81	553
PVX_116725	-0.0101	-0.0136	-0.0067	68	51	104	-0.0088	-0.015	-0.0027	78	46	253
PVX_058190	-0.0027	-0.0037	-0.0016	261	187	435	-0.0057	-0.009	-0.0023	123	77	304
PVX_098915	-0.004	-0.0069	-0.0012	171	100	599	-0.0084	-0.014	-0.0029	82	49	243

PVX_117880	-0.0021	-0.0028	-0.0014	335	248	513	-0.0021	-0.0033	-9.00E-04	327	210	744
PVX_090970	-0.0139	-0.0187	-0.0092	50	37	75	-0.0158	-0.023	-0.0086	44	30	81
PVX_099980	-0.0072	-0.0089	-0.0054	97	78	128	-0.012	-0.0155	-0.0085	58	45	82
PVX_114515	-0.0107	-0.0147	-0.0067	65	47	103	-0.01	-0.0151	-0.0048	70	46	145
PVX_082710	-0.0074	-0.0112	-0.0036	94	62	192	-0.0032	-0.0069	4.00E-04	214	101	Inf
PVX_084775	-0.0073	-0.0113	-0.0033	95	61	211	-0.0128	-0.0209	-0.0047	54	33	146
PVX_097710	-0.0077	-0.0119	-0.0035	90	58	198	-0.0053	-0.0104	-3.00E-04	130	66	2743
PVX_082430	-0.0115	-0.0169	-0.0061	60	41	114	-0.0063	-0.0118	-7.00E-04	111	59	1005
PVX_082670	-0.0069	-0.0093	-0.0045	101	74	155	-0.0107	-0.0156	-0.0058	65	44	119
PVX_002510	-0.0081	-0.0115	-0.0046	86	60	150	-0.0087	-0.0139	-0.0034	80	50	201
PVX_099975	-0.0103	-0.0148	-0.0058	67	47	119	-0.0057	-0.011	-4.00E-04	122	63	1654
PVX_101510	-0.0106	-0.0149	-0.0064	65	47	108	-0.0073	-0.0115	-0.003	95	60	231
PVX_003795	-0.0038	-0.0063	-0.0013	183	110	548	-0.0018	-0.0045	9.00E-04	389	154	Inf
PVX_089385	-0.0018	-0.0024	-0.0012	383	285	581	-0.002	-0.0031	-9.00E-04	342	222	742
PVX_084680	-0.0083	-0.0112	-0.0054	84	62	128	-0.0078	-0.0138	-0.0017	89	50	399
PVX_003905	-0.0135	-0.0183	-0.0086	52	38	80	-0.0067	-0.0133	-1.00E-04	104	52	11108
PVX_122580	-0.0087	-0.013	-0.0043	80	53	160	-0.0019	-0.0044	5.00E-04	360	159	Inf
PVX_100670	-0.0112	-0.0157	-0.0067	62	44	103	-0.0063	-0.0123	-2.00E-04	110	56	3053
PVX_087670	-0.0034	-0.0048	-0.002	203	143	347	-0.0081	-0.0136	-0.0027	85	51	256
PVX_088870	-0.0031	-0.0048	-0.0015	220	144	473	-0.0082	-0.0133	-0.003	85	52	227
PVX_109280	-0.0024	-0.0035	-0.0014	286	200	503	-0.004	-0.0065	-0.0015	173	106	471
PVX_082735	-0.0068	-0.0098	-0.0037	102	71	185	-0.0129	-0.0188	-0.007	54	37	100
PVX_119625	-0.0095	-0.0133	-0.0058	73	52	120	-0.0086	-0.0149	-0.0023	81	47	304
PVX_112665	-0.0134	-0.0207	-0.0061	52	34	115	-0.0123	-0.0203	-0.0044	56	34	159
PVX_091710-01	-0.0021	-0.0028	-0.0013	337	247	528	-0.0025	-0.0037	-0.0013	278	187	545
PVX_090275	-0.0019	-0.003	-9.00E-04	358	232	785	-0.0041	-0.0068	-0.0014	168	102	482
PVX_123975	-0.0124	-0.0178	-0.007	56	39	99	-0.0023	-0.0059	0.0013	301	118	Inf
PVX_110960	-0.0082	-0.0113	-0.0051	85	61	137	-0.0029	-0.0075	0.0018	240	92	Inf
PVX_003520	-0.0079	-0.0118	-0.0039	88	59	180	-0.0022	-0.0059	0.0016	319	117	Inf

PVX_080305	-0.0076	-0.0109	-0.0043	92	64	162	-0.0043	-0.0082	-4.00E-04	162	85	1908
PVX_114620	-0.0091	-0.0132	-0.0049	77	52	143	-0.0081	-0.014	-0.0022	86	49	320
PVX_081550	-0.007	-0.0105	-0.0034	99	66	204	-0.0055	-0.0101	-8.00E-04	126	68	840
PVX_081845	-0.0062	-0.0091	-0.0034	111	76	202	-0.0092	-0.0147	-0.0037	75	47	188
PVX_079980	-0.0102	-0.0139	-0.0066	68	50	106	-0.0059	-0.0107	-0.0011	117	65	605
PVX_096990	-0.0065	-0.0091	-0.0039	107	76	177	-0.0066	-0.0112	-0.002	105	62	350
PVX_001725	-0.0022	-0.003	-0.0014	314	229	500	-0.0029	-0.0047	-0.0012	236	147	586
PVX_095035-01	-0.0074	-0.0124	-0.0024	94	56	295	-0.0017	-0.0048	0.0015	412	144	Inf
PVX_067190	-0.0024	-0.0043	-5.00E-04	286	161	1266	-0.0011	-0.0028	6.00E-04	631	244	Inf
PVX_116825	-0.0031	-0.0043	-0.0019	225	162	370	-0.0106	-0.0177	-0.0035	65	39	198
PVX_117880	-0.0021	-0.0028	-0.0014	335	248	513	-0.0021	-0.0033	-9.00E-04	327	210	744
PVX_087915	-0.0044	-0.0086	-3.00E-04	156	81	2185	-0.0039	-0.0084	6.00E-04	177	83	Inf
PVX_082685	-0.0072	-0.0116	-0.0029	96	60	243	-0.012	-0.0184	-0.0055	58	38	125
PVX_001975	-0.011	-0.0166	-0.0054	63	42	128	-0.0043	-0.0094	7.00E-04	160	74	Inf
PVX_097590	-0.0066	-0.0104	-0.0029	105	67	243	-0.0026	-0.0053	1.00E-04	270	132	Inf
PVX_092615	-0.0059	-0.0084	-0.0034	117	82	204	-0.0098	-0.0154	-0.0041	71	45	169
PVX_097720	-0.0026	-0.0035	-0.0018	263	198	389	-0.0031	-0.0046	-0.0015	225	149	459
PVX_091990	-0.0052	-0.007	-0.0034	134	100	206	-0.0081	-0.013	-0.0032	86	53	218
PVX_082665	-0.004	-0.0054	-0.0025	174	128	274	-0.0071	-0.0107	-0.0035	98	65	199
PVX_089845	-0.0092	-0.0133	-0.005	76	52	138	-0.0032	-0.0065	1.00E-04	216	106	Inf
PVX_099975	-0.0103	-0.0148	-0.0058	67	47	119	-0.0057	-0.011	-4.00E-04	122	63	1654
PVX_112670	-0.0011	-0.0016	-5.00E-04	650	428	1350	-0.0022	-0.0031	-0.0012	317	221	563
PVX_097745	-0.0026	-0.0049	-3.00E-04	267	143	2052	-0.0013	-0.0025	0	552	276	275058
PVX_003555-1	-0.0036	-0.005	-0.0021	195	140	323	-0.006	-0.0097	-0.0023	115	71	302
PVX_084475-01	-0.0097	-0.0133	-0.0062	71	52	112	-0.014	-0.0223	-0.0058	49	31	120
PVX_001020	-0.0118	-0.0161	-0.0074	59	43	93	-0.0037	-0.0073	-1.00E-04	187	95	5145
PVX_094690	-0.0029	-0.0037	-0.0021	241	188	338	-0.0021	-0.0032	-0.001	329	214	713
PVX_090270	-0.0065	-0.0089	-0.0041	107	78	171	-0.007	-0.0112	-0.0028	99	62	247
PVX_119230	-0.0102	-0.0142	-0.0062	68	49	112	-0.0016	-0.0039	7.00E-04	421	176	Inf

PVX_118680	-0.0105	-0.0145	-0.0064	66	48	108	-0.0054	-0.0102	-6.00E-04	128	68	1117
PVX_101525	-0.0029	-0.0043	-0.0014	243	160	501	-0.0037	-0.0075	1.00E-04	187	93	Inf
PVX_119355	-0.0067	-0.0097	-0.0036	104	72	191	-0.0065	-0.012	-0.0011	106	58	652
PVX_121920	-0.0081	-0.0116	-0.0046	85	60	149	-0.0056	-0.0104	-8.00E-04	124	67	863
PVX_125730	-0.0079	-0.0112	-0.0045	88	62	153	-0.0102	-0.0161	-0.0043	68	43	160
PVX_091710-02	-0.0097	-0.0133	-0.0061	71	52	113	-0.0124	-0.0184	-0.0065	56	38	107
PVX_092990	-0.0034	-0.0047	-0.0021	204	147	332	-0.0039	-0.0064	-0.0014	176	108	483
PVX_122865	-0.0115	-0.0162	-0.0067	61	43	104	-0.0045	-0.0091	0	153	76	Inf
PVX_001715	-0.0045	-0.0064	-0.0027	153	109	258	-0.0075	-0.0129	-0.0021	92	54	332
PVX_082595	-0.0086	-0.0116	-0.0056	80	60	123	-0.0069	-0.0121	-0.0017	101	57	416
PVX_094310	-0.0098	-0.0144	-0.0053	71	48	132	-0.0069	-0.0121	-0.0018	100	57	385
PVX_122965	-0.0057	-0.0096	-0.0018	121	72	387	-0.005	-0.0092	-7.00E-04	140	75	1023
PVX_095435	-1.00E-04	-4.00E-04	1.00E-04	5477	1767	Inf	-2.00E-04	-6.00E-04	2.00E-04	3629	1212	Inf
PVX_096020	-0.01	-0.0134	-0.0066	69	52	105	-0.0128	-0.0201	-0.0055	54	35	127
PVX_080120	-0.0128	-0.0167	-0.0088	54	41	78	-0.0104	-0.0165	-0.0042	67	42	166
PVX_121910	-0.0022	-0.003	-0.0015	310	232	469	-0.0027	-0.0041	-0.0013	257	170	522
PVX_094920	-0.0024	-0.0031	-0.0016	293	222	430	-0.0042	-0.0065	-0.0019	166	107	371
PVX_095035-02	-0.0029	-0.0052	-6.00E-04	241	134	1196	-0.0015	-0.0043	0.0013	461	161	Inf
PVX_102635	-0.0032	-0.0044	-0.002	219	159	353	-0.0069	-0.0109	-0.0029	100	64	239
PVX_099705	-0.0039	-0.0067	-0.0011	178	103	657	-0.0012	-0.0034	0.001	580	205	Inf
PVX_117880	-0.0021	-0.0028	-0.0014	335	248	513	-0.0021	-0.0033	-9.00E-04	327	210	744
PVX_097577	-0.0056	-0.0089	-0.0023	123	78	297	-0.0017	-0.0051	0.0016	399	136	Inf
PVX_080100	-0.0029	-0.0039	-0.002	236	178	353	-0.0071	-0.0118	-0.0024	97	59	288
PVX_081760	-0.0099	-0.0137	-0.0062	70	51	111	-0.0073	-0.0126	-0.002	95	55	344
PVX_003985	-0.0059	-0.0087	-0.0031	117	79	223	-0.0113	-0.0166	-0.0059	61	42	117
PVX_111065	-0.0063	-0.0091	-0.0036	109	76	194	-0.0171	-0.0244	-0.0097	41	28	71
PVX_097725	-0.0074	-0.0108	-0.004	94	64	173	-0.0176	-0.0245	-0.0107	39	28	65
PVX_088910	-0.0076	-0.0102	-0.0049	92	68	142	-0.0146	-0.0209	-0.0084	47	33	82
PVX_082655	-0.0038	-0.0051	-0.0025	181	135	277	-0.0086	-0.0126	-0.0045	81	55	152

PVX_079800	-0.0072	-0.0109	-0.0036	96	64	191	-0.0075	-0.0133	-0.0018	92	52	396
PVX_097625	-0.0041	-0.0055	-0.0027	169	127	254	-0.0093	-0.013	-0.0057	74	53	121
PVX_096055	-0.0012	-0.0018	-6.00E-04	580	394	1102	-0.002	-0.0029	-0.001	354	238	690
PVX_115030	-4.00E-04	-0.0012	4.00E-04	1602	566	Inf	-0.0024	-0.0049	1.00E-04	293	142	Inf
PVX_084475-02	-0.0111	-0.0165	-0.0056	63	42	123	-0.0085	-0.0136	-0.0034	82	51	206
PVX_001715	-0.0045	-0.0064	-0.0027	153	109	258	-0.0075	-0.0129	-0.0021	92	54	332
PVX_093680	-0.0118	-0.0179	-0.0058	59	39	119	-0.0024	-0.0049	1.00E-04	286	141	Inf
PVX_090250	-0.0037	-0.0067	-8.00E-04	187	104	904	-0.0016	-0.0034	3.00E-04	444	204	Inf
PVX_084110	-0.0062	-0.0094	-0.003	111	73	231	-0.0014	-0.0034	7.00E-04	504	201	Inf
PVX_099975	-0.0103	-0.0148	-0.0058	67	47	119	-0.0057	-0.011	-4.00E-04	122	63	1654
PVX_116850	-0.0029	-0.0041	-0.0018	237	169	394	-0.0068	-0.0106	-0.0029	103	65	239
PVX_111175	-0.0062	-0.0105	-0.0019	112	66	362	-0.0032	-0.0077	0.0014	219	90	Inf
PVX_098585	-0.0015	-0.0022	-8.00E-04	472	317	923	-0.0025	-0.0038	-0.0012	275	183	558
PVX_096995	-0.0128	-0.0176	-0.0081	54	39	86	-0.0209	-0.0273	-0.0145	33	25	48
PVX_122805-01	-0.0045	-0.0073	-0.0017	154	95	402	-0.002	-0.0052	0.0012	344	133	Inf
PVX_097575	-0.0096	-0.0138	-0.0053	73	50	131	-0.0068	-0.0142	6.00E-04	102	49	Inf
PVX_002790	-0.0018	-0.0033	-2.00E-04	396	211	3094	-0.006	-0.01	-0.002	115	70	340
PVX_121950	-0.0074	-0.0108	-0.0039	94	64	178	-0.003	-0.0068	9.00E-04	235	102	Inf
PVX_092990	-0.0034	-0.0047	-0.0021	204	147	332	-0.0039	-0.0064	-0.0014	176	108	483
PVX_083275	-0.0013	-0.0026	1.00E-04	539	262	Inf	-0.0021	-0.0043	1.00E-04	331	161	Inf
PVX_124090	-0.0169	-0.0236	-0.0101	41	29	68	-0.014	-0.0214	-0.0066	49	32	105
PVX_095055	-0.0087	-0.0129	-0.0045	80	54	155	-0.001	-0.0031	0.0012	714	220	Inf
PVX_114025	-0.0021	-0.0029	-0.0013	336	243	546	-0.0027	-0.0043	-0.0012	252	162	572
PVX_101580	-0.0058	-0.0093	-0.0024	119	75	290	-0.0016	-0.0073	0.0041	439	96	Inf
PVX_094920	-0.0024	-0.0031	-0.0016	293	222	430	-0.0042	-0.0065	-0.0019	166	107	371
PVX_084340	-0.004	-0.0057	-0.0023	174	122	306	-0.0075	-0.0115	-0.0034	93	60	203
PVX_123575	-0.0123	-0.0167	-0.008	56	42	87	-0.0076	-0.0137	-0.0016	91	51	436
PVX_082640	-0.0051	-0.0082	-0.0021	135	84	336	-0.0017	-0.0047	0.0013	414	148	Inf
PVX_121925	-0.0118	-0.0168	-0.0068	59	41	102	-0.0022	-0.0066	0.0022	315	105	Inf

PVX_112690	-0.0027	-0.0035	-0.0019	255	198	358	-0.0023	-0.0037	-9.00E-04	301	186	788
PVX_080100	-0.0029	-0.0039	-0.002	236	178	353	-0.0071	-0.0118	-0.0024	97	59	288
PVX_121897	-0.0036	-0.0052	-0.0019	195	134	358	-0.008	-0.0129	-0.0031	86	54	221
PVX_097680	-0.0066	-0.0099	-0.0033	105	70	210	-0.0092	-0.0136	-0.0047	76	51	147
PVX_086915	-0.0041	-0.0075	-7.00E-04	169	92	1015	-0.0015	-0.0039	8.00E-04	450	178	Inf
PVX_082700	-0.0049	-0.0073	-0.0024	142	95	284	-0.0135	-0.0201	-0.0069	51	35	100
PVX_088910-Tr1	-0.0037	-0.0064	-0.001	188	109	669	-0.002	-0.0053	0.0013	343	130	Inf
PVX_082650	-0.0059	-0.0082	-0.0035	118	84	198	-0.0153	-0.0225	-0.008	45	31	87
PVX_085665	-0.0041	-0.0075	-7.00E-04	169	92	1032	-0.0012	-0.0026	1.00E-04	574	272	Inf
PVX_115165	-0.0031	-0.0053	-9.00E-04	224	131	777	-0.0029	-0.0056	-2.00E-04	239	125	2899
PVX_112680	-0.0017	-0.0025	-9.00E-04	417	281	807	-0.0021	-0.0032	-9.00E-04	336	215	767
PVX_081815	-0.0051	-0.0082	-0.0021	135	85	326	-0.0011	-0.0038	0.0015	605	181	Inf
PVX_003905	-0.0135	-0.0183	-0.0086	52	38	80	-0.0067	-0.0133	-1.00E-04	104	52	11108
PVX_123760	-0.0162	-0.0213	-0.0111	43	33	63	-0.0067	-0.0133	-1.00E-04	103	52	8774
PVX_085550	-0.0061	-0.0097	-0.0026	113	72	267	-0.0026	-0.0071	0.002	271	97	Inf
PVX_083570	-0.003	-0.0051	-8.00E-04	234	137	816	-0.0011	-0.0035	0.0012	612	199	Inf
PVX_098582	-0.0054	-0.0084	-0.0024	129	82	292	-0.0021	-0.0044	2.00E-04	328	158	Inf
PVX_116915	-0.0069	-0.0104	-0.0033	101	67	209	-0.0054	-0.0092	-0.0016	128	75	427
PVX_099975	-0.0103	-0.0148	-0.0058	67	47	119	-0.0057	-0.011	-4.00E-04	122	63	1654
PVX_085930	-0.0025	-0.0035	-0.0016	276	201	440	-0.0031	-0.0047	-0.0015	226	148	477
PVX_084420	-0.0059	-0.0087	-0.0031	117	79	225	-0.0073	-0.0116	-0.0029	95	60	237
PVX_002500	-0.0096	-0.0138	-0.0055	72	50	127	-0.0124	-0.0191	-0.0058	56	36	120
PVX_122805-02	-0.0104	-0.0136	-0.0073	67	51	95	-0.0115	-0.0173	-0.0057	60	40	122
PVX_115465	-0.0107	-0.0145	-0.0069	65	48	100	-0.0082	-0.0152	-0.0012	85	46	602
PVX_081330	-0.0149	-0.0199	-0.0099	46	35	70	-0.0064	-0.0108	-0.0019	109	64	372
PVX_003565	-0.0022	-0.0047	3.00E-04	316	148	Inf	-6.00E-04	-0.0015	2.00E-04	1107	467	Inf
PVX_092975	-0.01	-0.0136	-0.0064	69	51	108	-0.002	-0.0045	6.00E-04	355	154	Inf
PVX_088860	-0.0049	-0.0068	-0.003	142	102	234	-0.0056	-0.0088	-0.0024	124	79	287
PVX_084815	-0.0081	-0.012	-0.0043	85	58	162	-0.015	-0.0221	-0.0079	46	31	87

PVX_095055	-0.0087	-0.0129	-0.0045	80	54	155	-0.001	-0.0031	0.0012	714	220	Inf
PVX_099900	-0.0124	-0.0173	-0.0075	56	40	93	-0.0022	-0.0056	0.0013	322	124	Inf
PVX_086320	-0.0039	-0.0066	-0.0013	176	105	535	-0.0015	-0.0037	7.00E-04	454	185	Inf
PVX_112710	-0.0107	-0.0161	-0.0053	65	43	130	-0.0027	-0.0069	0.0016	260	101	Inf
PVX_111215	-0.0112	-0.0169	-0.0055	62	41	127	-0.0014	-0.0048	0.0019	479	145	Inf
PVX_119265	-0.0026	-0.0037	-0.0016	265	188	445	-0.0027	-0.0045	-0.001	253	155	692
PVX_122720	-0.0021	-0.0045	2.00E-04	326	154	Inf	-0.0011	-0.0037	0.0014	605	186	Inf
PVX_002800	-0.0059	-0.0096	-0.0022	118	73	317	-0.0029	-0.008	0.0022	241	87	Inf
PVX_003745	-0.0019	-0.0028	-9.00E-04	372	248	745	-0.0035	-0.0058	-0.0012	198	120	571
PVX_101515	-0.0074	-0.0107	-0.0041	93	65	169	-0.0109	-0.0171	-0.0048	63	41	144
PVX_088125	-0.0092	-0.0124	-0.0061	75	56	113	-0.0134	-0.0197	-0.0072	52	35	96
PVX_125728	-0.0023	-0.0033	-0.0014	295	212	485	-0.003	-0.0052	-8.00E-04	230	132	890
PVX_097690	-0.0062	-0.0094	-0.0031	111	74	222	-0.0099	-0.0166	-0.0032	70	42	215
PVX_090230	-0.0045	-0.0064	-0.0025	156	108	280	-0.006	-0.01	-0.002	115	69	340
PVX_082695	-0.0074	-0.013	-0.0018	94	53	396	-0.0034	-0.0081	0.0013	203	86	Inf
PVX_096245-Tr1	-0.0041	-0.0068	-0.0013	170	102	518	-0.0011	-0.0028	6.00E-04	635	248	Inf
PVX_082645	-0.0083	-0.0116	-0.0049	84	60	140	-0.01	-0.015	-0.0049	70	46	141
PVX_000930	-0.0024	-0.0034	-0.0015	283	206	456	-0.0039	-0.0058	-0.0021	177	120	332
PVX_080530	-0.0097	-0.0152	-0.0042	72	46	165	-0.0026	-0.0055	3.00E-04	264	125	Inf
PVX_117880	-0.0021	-0.0028	-0.0014	335	248	513	-0.0021	-0.0033	-9.00E-04	327	210	744
PVX_087095	5.00E-04	-0.0012	0.0022	Inf	598	Inf	-4.00E-04	-0.0021	0.0014	1968	324	Inf
PVX_003905	-0.0135	-0.0183	-0.0086	52	38	80	-0.0067	-0.0133	-1.00E-04	104	52	11108
PVX_099295	-0.0018	-0.0024	-0.0012	378	284	568	-0.0017	-0.0027	-7.00E-04	402	255	956
PVX_085550	-0.0061	-0.0097	-0.0026	113	72	267	-0.0026	-0.0071	0.002	271	97	Inf
PVX_084470	-0.009	-0.0129	-0.0051	77	54	137	-0.0124	-0.0193	-0.0055	56	36	126
PVX_098582	-0.0054	-0.0084	-0.0024	129	82	292	-0.0021	-0.0044	2.00E-04	328	158	Inf
PVX_096950	-0.0086	-0.0115	-0.0056	81	60	124	-0.0117	-0.0184	-0.0049	59	38	141
PVX_099975	-0.0103	-0.0148	-0.0058	67	47	119	-0.0057	-0.011	-4.00E-04	122	63	1654
PVX_087885	-0.0022	-0.003	-0.0013	321	232	520	-0.0035	-0.0052	-0.0018	198	133	385

PVX_110810	-0.0038	-0.005	-0.0026	182	139	267	-0.0068	-0.0111	-0.0025	102	62	281
PVX_090240	-0.0057	-0.0082	-0.0032	121	84	215	-0.0097	-0.0174	-0.0021	71	40	336
PVX_088820	-0.0039	-0.0051	-0.0027	178	136	259	-0.0052	-0.008	-0.0023	134	87	297
PVX_094830	-0.003	-0.0041	-0.0019	230	169	364	-0.0051	-0.0077	-0.0026	135	90	268
PVX_083550	-0.0084	-0.013	-0.0038	82	53	182	-0.0029	-0.0071	0.0014	242	98	Inf
PVX_111035	-0.0113	-0.0166	-0.0059	61	42	117	-0.0083	-0.014	-0.0026	84	49	269
PVX_094255	-0.0039	-0.0053	-0.0025	178	130	281	-0.0131	-0.0202	-0.0059	53	34	117
PVX_097715	-0.0061	-0.0078	-0.0044	113	89	156	-0.0088	-0.0137	-0.0038	79	50	182
PVX_088990	-0.0039	-0.0063	-0.0015	179	110	475	-0.002	-0.0047	8.00E-04	354	148	Inf
PVX_090030	-0.0056	-0.0088	-0.0023	124	79	297	-0.0065	-0.0109	-0.0021	106	63	329
PVX_090210	-3.00E-04	-8.00E-04	3.00E-04	2482	822	Inf	-8.00E-04	-0.0019	3.00E-04	885	369	Inf
PVX_101605	-0.0065	-0.0098	-0.0031	107	70	225	-0.0012	-0.0035	0.0011	570	198	Inf
PVX_110945	-0.0126	-0.0172	-0.0081	55	40	86	-0.0061	-0.0122	0	114	57	Inf
PVX_086850	-0.0059	-0.0089	-0.0029	117	78	236	-0.001	-0.0026	5.00E-04	662	265	Inf
PVX_111290	-0.0029	-0.0051	-7.00E-04	239	137	957	-0.0026	-0.0056	4.00E-04	265	123	Inf
PVX_093665	-0.003	-0.0055	-5.00E-04	233	127	1502	-0.0011	-0.0029	6.00E-04	607	241	Inf
PVX_117465	-0.0135	-0.0187	-0.0083	51	37	84	-0.0027	-0.0071	0.0018	260	98	Inf
PVX_092915	-0.0075	-0.0107	-0.0043	93	65	162	-0.0079	-0.0136	-0.0022	88	51	322
PVX_090265	-0.0052	-0.0078	-0.0027	132	89	257	-0.0095	-0.0155	-0.0035	73	45	195
PVX_084335	-0.0117	-0.0157	-0.0077	59	44	90	-0.0072	-0.0132	-0.0011	97	52	609
PVX_123505	-9.00E-04	-0.0029	0.0012	807	236	Inf	-0.0014	-0.0034	6.00E-04	499	203	Inf
PVX_097695	-0.0039	-0.0066	-0.0013	177	106	538	-0.0103	-0.0153	-0.0053	67	45	131
PVX_001005	-0.0115	-0.0172	-0.0057	61	40	122	-0.0023	-0.0057	0.0011	302	122	Inf
PVX_082690	-0.0081	-0.0126	-0.0036	86	55	192	-0.0036	-0.0074	3.00E-04	195	93	Inf
PVX_092425	-0.0046	-0.0075	-0.0018	149	92	396	-0.0013	-0.0033	7.00E-04	521	208	Inf
PVX_099975	-0.0103	-0.0148	-0.0058	67	47	119	-0.0057	-0.011	-4.00E-04	122	63	1654
PVX_091700	-0.0111	-0.0164	-0.0057	63	42	121	-0.0077	-0.0128	-0.0026	90	54	263
PVX_097960	-0.0026	-0.0047	-5.00E-04	264	146	1361	-0.002	-0.0049	0.001	352	141	Inf
PVX_003555-2	-0.0011	-0.0016	-5.00E-04	654	423	1434	-0.0018	-0.0026	-9.00E-04	390	262	763

PVX_099375	-0.0138	-0.0181	-0.0095	50	38	73	-0.0031	-0.007	8.00E-04	223	99	Inf
PVX_003905	-0.0135	-0.0183	-0.0086	52	38	80	-0.0067	-0.0133	-1.00E-04	104	52	11108
PVX_123685-01	-0.0137	-0.0185	-0.0088	51	37	79	-0.0101	-0.0168	-0.0033	69	41	207
PVX_000975	-0.0087	-0.0127	-0.0047	80	55	148	-0.0033	-0.0076	0.001	212	92	Inf
PVX_086090	-0.0076	-0.0122	-0.0031	91	57	227	-0.0014	-0.0037	0.001	513	186	Inf
PVX_125738	-0.003	-0.0043	-0.0016	235	161	436	-0.0058	-0.0095	-0.0022	119	73	312
PVX_112685	-0.0029	-0.004	-0.0018	239	174	383	-0.003	-0.0047	-0.0013	232	147	544
PVX_099975	-0.0103	-0.0148	-0.0058	67	47	119	-0.0057	-0.011	-4.00E-04	122	63	1654
PVX_099930	-0.0043	-0.0065	-0.0021	162	107	335	-0.01	-0.017	-0.0029	69	41	235
PVX_110810	-0.0038	-0.005	-0.0026	182	139	267	-0.0068	-0.0111	-0.0025	102	62	281
PVX_087725	-0.0093	-0.0133	-0.0052	75	52	133	-0.0037	-0.0094	0.0021	189	73	Inf
PVX_088825	-0.0086	-0.013	-0.0041	81	53	169	-0.0052	-0.0104	1.00E-04	135	67	Inf
PVX_001015	-0.0033	-0.0049	-0.0016	212	141	427	-0.0092	-0.0154	-0.003	75	45	229
PVX_092995	-0.0099	-0.0128	-0.007	70	54	99	-0.016	-0.0241	-0.008	43	29	87
PVX_114330	-0.0122	-0.0176	-0.0069	57	39	101	-0.016	-0.0243	-0.0076	43	29	91
PVX_090330	-0.0023	-0.0032	-0.0013	308	218	521	-0.0035	-0.0055	-0.0015	200	127	470
PVX_003770	-0.0116	-0.0152	-0.008	60	46	87	-0.0158	-0.0218	-0.0099	44	32	70
PVX_089940	-0.0055	-0.009	-0.0021	125	77	336	-0.0011	-0.0028	7.00E-04	653	245	Inf
PVX_090225	-0.0018	-0.0027	-0.001	379	257	722	-0.0042	-0.0062	-0.0022	164	111	312
PVX_000810	-0.021	-0.0295	-0.0125	33	23	55	-0.0304	-0.038	-0.0227	23	18	31
PVX_099575	-0.0111	-0.0197	-0.0025	63	35	283	-0.0249	-0.0292	-0.0206	28	24	34
PVX_114565	-0.0021	-0.0055	0.0013	330	127	Inf	-0.0078	-0.0113	-0.0043	89	62	160
PVX_100975	-0.0132	-0.0193	-0.0071	53	36	98	-0.0276	-0.0337	-0.0216	25	21	32
PVX_118040	-0.0163	-0.0244	-0.0083	42	28	84	-0.0197	-0.0231	-0.0163	35	30	43
PVX_089585	-0.0208	-0.0302	-0.0114	33	23	61	-0.0221	-0.0261	-0.0181	31	27	38
PVX_081560	-0.018	-0.0256	-0.0103	39	27	67	-0.0293	-0.0342	-0.0244	24	20	28
PVX_000815	-0.0181	-0.025	-0.0113	38	28	61	-0.032	-0.0366	-0.0274	22	19	25
PVX_113965_1o2	-0.015	-0.0229	-0.0071	46	30	98	-0.0272	-0.0329	-0.0214	26	21	32
PVX_113965_2o2	-0.0137	-0.0287	0.0012	51	24	Inf	-0.0295	-0.0364	-0.0226	24	19	31

PVX_123510	-0.0131	-0.0212	-0.0051	53	33	137	-0.034	-0.0404	-0.0275	20	17	25
PVX_083025	-0.0091	-0.0145	-0.0036	76	48	193	-0.027	-0.0333	-0.0207	26	21	33
PVX_084410	-0.0157	-0.0287	-0.0027	44	24	256	-0.0338	-0.0391	-0.0284	21	18	24
PVX_001025	NA	NA	NA	NA	NA	NA	-0.0211	-0.0263	-0.0159	33	26	44
PVX_119755	-0.0159	-0.0238	-0.0079	44	29	87	-0.0262	-0.0302	-0.0222	26	23	31
PVX_083235	-0.0188	-0.0254	-0.0121	37	27	57	-0.0425	-0.0524	-0.0326	16	13	21
PVX_094925	-0.019	-0.0262	-0.0118	37	26	59	-0.0233	-0.0288	-0.0177	30	24	39
PVX_112625	-0.0143	-0.0216	-0.007	49	32	99	-0.03	-0.0334	-0.0267	23	21	26
PVX_092745	-0.0097	-0.0179	-0.0015	71	39	453	-0.0244	-0.0277	-0.021	28	25	33
PVX_079955	-0.0113	-0.0198	-0.0027	62	35	257	-0.0165	-0.021	-0.0121	42	33	57
PVX_086010	-0.0118	-0.0205	-0.0031	59	34	226	-0.0497	-0.0557	-0.0438	14	12	16
PVX_099080	-0.0106	-0.0179	-0.0034	65	39	205	-0.0306	-0.0374	-0.0239	23	19	29
PVX_081705	-0.008	-0.0123	-0.0038	86	57	183	-0.0242	-0.0287	-0.0198	29	24	35
PVX_101345	-0.0176	-0.0286	-0.0065	39	24	106	-0.0374	-0.0439	-0.0309	19	16	22
PVX_100755	-0.0075	-0.0128	-0.0023	92	54	305	-0.0364	-0.0419	-0.0309	19	17	22
PVX_000555	-0.0075	-0.0139	-0.0012	92	50	598	-0.0186	-0.0224	-0.0149	37	31	47
PVX_123705	-0.0154	-0.0227	-0.0082	45	31	85	-0.0306	-0.0343	-0.027	23	20	26
PVX_079880	-0.0294	-0.0363	-0.0225	24	19	31	-0.0456	-0.0519	-0.0393	15	13	18
PVX_099315	-0.0125	-0.0196	-0.0054	55	35	127	-0.0363	-0.0406	-0.0321	19	17	22
PVX_001000	-0.0171	-0.0237	-0.0105	41	29	66	-0.029	-0.0343	-0.0238	24	20	29
PVX_123105	-0.0113	-0.0181	-0.0044	61	38	157	-0.0212	-0.025	-0.0173	33	28	40
PVX_117195	-0.0219	-0.0286	-0.0152	32	24	46	-0.0333	-0.0394	-0.0271	21	18	26
PVX_002550_1o3	-0.0518	-0.0656	-0.0381	13	11	18	-0.0186	-0.0227	-0.0144	37	31	48
PVX_002550_2o3	-0.0118	-0.0167	-0.0069	59	42	100	-0.0438	-0.0531	-0.0345	16	13	20
PVX_002550_3o3	-0.0114	-0.0161	-0.0067	61	43	104	-0.0145	-0.0181	-0.0108	48	38	64

Table S2. Purified *P. vivax* proteins used in the validation phase and their individual performance, complete list. Area under the curve (AUC) from the single antigen classifier is shown; proteins are listed in order of best performance. All 60 proteins are shown; Table 2 in the main manuscript included the first 8 proteins. References listed are for the protein production and purification method.

Protein ID[a]	Gene Annotation[a]	Short code	Protein length, aa	Construct, aa (size)	Expression System[c]	Purification Method	AUC: all samples	AUC: Thailand	AUC: Brazil	AUC: Solomons
PVX_094255B	reticulocyte binding protein 2b (RBP2b)	W50	2806	161-1454 (1294)	*E. coli*	2x affinity + size exclusion (*1*)	0.816	0.829	0.787	0.866
PVX_094255A	reticulocyte binding protein 2b (RBP2b)	W20	2806	1986-2653 (667)	WGCF	One-step Ni column	0.748	0.786	0.717	0.733
PVX_087885B	rhoptry-associated membrane antigen, putative	W47	730	462-730 (269)	WGCF	One-step Ni column (*2*)	0.728	0.777	0.664	0.565
PVX_099980	merozoite surface protein 1 (MSP1-19)	W01	1751	1622-1729 (108)	WGCF	One-step Ni column	0.713	0.800	0.741	0.736
PVX_112670	unspecified product	W08	335	34-end (302)	WGCF	One-step Ni column	0.698	0.750	0.718	0.621
PVX_092995	tryptophan-rich antigen (Pv-fam-a)	W46	385	25-358 (334)	WGCF	One-step Ni column (*2*)	0.689	0.741	0.707	0.676
PVX_096995	tryptophan-rich antigen (Pv-fam-a)	W02	480	61-end (420)	WGCF	One-step Ni column	0.689	0.772	0.623	0.532
PVX_121920	reticulocyte binding protein 2a (RBP2a)	W49	2487	160-1135 (976)	*E. coli*	2x affinity + size exclusion (*1*)	0.685	0.690	0.699	0.647
KMZ83376.1[b]	erythrocyte binding protein II (PvEBPII)	W58	786	109-432 (324)	*E. coli*	Ni, ion exchange, gel filtration (*4, 5*)	0.684	0.763	0.718	0.687
PVX_097625	merozoite surface protein 8 (MSP8), putative	W30	487	24-463 (440)	WGCF	One-step Ni column	0.681	0.759	0.721	0.696
PVX_087885A	rhoptry associated membrane antigen, putative	W16	730	462-730 (269)	WGCF	One-step Ni column	0.680	0.739	0.723	0.668
PVX_003770	merozoite surface protein 5 (MSP5)	W12	387	23-365 (343)	WGCF	One-step Ni column	0.670	0.729	0.649	0.552
PVX_097720	merozoite surface protein 3 (MSP3.10)	W39	852	25-end (828)	WGCF	One-step Ni column	0.670	0.780	0.713	0.693
PVX_084720	translocon component PTEX150, putative	W11	908	24-908 (885)	WGCF	One-step Ni column	0.668	0.725	0.625	0.487
PVX_000930	sexual stage antigen s16, putative	W40	140	31-end (110)	WGCF	One-step Ni column	0.665	0.773	0.755	0.682
PVX_082700	merozoite surface protein 7 (MSP7.1)	W27	420	23-end (397)	WGCF	One-step Ni column	0.664	0.721	0.701	0.631
PVX_088820B	tryptophan-rich antigen (Pv-fam-a)	W44	316	58-end (259)	WGCF	One-step Ni column (*2*)	0.663	0.685	0.570	0.507
PVX_082670	merozoite surface protein 7 (MSP7), putative	W31	411	24-end (388)	WGCF	One-step Ni column	0.660	0.698	0.679	0.672
PVX_095055	Rh5 interacting protein, putative (RIPR)	W55	1075	552-1075 (524)	*E. coli*	2x affinity + size exclusion (*3*)	0.658	0.741	0.745	0.712
PVX_003555	Plasmodium exported protein, unknown function	W17	1122	434-1075 (642)	WGCF	One-step Ni column	0.647	0.722	0.732	0.604
PVX_097715	hypothetical protein	W05	450	20-end (431)	WGCF	One-step Ni column	0.647	0.660	0.575	0.466
AAY34130.1[b]	Duffy binding protein (DBP, region 2, AH strain)	W57	237	1-237 (237)	*E. coli*	Ni, ion exchange, gel filtration (*4*)	0.640	0.708	0.730	0.656
PVX_112690	unspecified product	W14	313	30-313 (284)	WGCF	One-step Ni column	0.639	0.674	0.608	0.494
PVX_090265	tryptophan-rich antigen (Pv-fam-a)	W26	326	1-326 (326)	WGCF	One-step Ni column	0.635	0.762	0.706	0.692
PVX_110810B	Duffy binding protein (DBP, region 3-5, Sal1 strain)	W60	1070	508-899 (392)	*E. coli*	One-step Ni column (*3*)	0.630	0.703	0.727	0.676
PVX_098585	reticulocyte binding protein 1a (RBP1a)	W59	2833	160-1170 (1011)	*E. coli*	2x affinity + size exclusion (*1*)	0.618	0.673	0.666	0.609

PVX_117385	phosphatidylinositol-4-phosphate-5-kinase, putative	W18	326	1-326 (326)	WGCF	One-step Ni column	0.611	0.653	0.559	0.499
PVX_091710	hypothetical protein, conserved	W15	1689	26-884 (859)	WGCF	One-step Ni column	0.608	0.717	0.582	0.520
PVX_099930B	high molecular weight rhoptry protein 2 (RhopH2)	W42	1369	23-387 (365)	WGCF	One-step Ni column (*2*)	0.607	0.663	0.632	0.626
PVX_082735	thrombospondin-related anonymous protein (TRAP)	W34	556	26-493 (468)	WGCF	One-step Ni column	0.607	0.678	0.570	0.489
PVX_098582	reticulocyte binding protein 1b (RBP1b)	W48	2608	140-1275 (1136)	*E. coli*	2x affinity + size exclusion (*1*)	0.602	0.579	0.627	0.557
PVX_001000	hypothetical protein, conserved	W29	668	20-end (650)	WGCF	One-step Ni column	0.601	0.656	0.589	0.612
PVX_090325	reticulocyte binding protein 2c (RBP2c non binding region)	W51	2824	501-1300 (800)	*E. coli*	2x affinity + size exclusion (*1*)	0.601	0.735	0.683	0.630
PVX_099930A	high molecular weight rhoptry protein 2 (RhopH2)	W32	1369	23-387 (365)	WGCF	One-step Ni column	0.594	0.652	0.654	0.563
PVX_090970	hypothetical protein, conserved	W10	266	20-254 (235)	WGCF	One-step Ni column	0.593	0.686	0.613	0.599
PVX_082645	merozoite surface protein 7 (MSP7), putative	W35	377	23-end (355)	WGCF	One-step Ni column	0.590	0.672	0.607	0.631
PVX_084340	IMP-specific 5'-nucleotidase, putative	W33	444	1-444 (444)	WGCF	One-step Ni column	0.589	0.666	0.559	0.592
PVX_110810A	Duffy binding protein (DBP, region 2, Sal1 strain)	W53	1070	193-521 (329)	*E. coli*	Ni, ion exchange, gel filtration (*4, 5*)	0.582	0.682	0.648	0.655
PVX_112680	unspecified product	W04	313	33-end (281)	WGCF	One-step Ni column	0.580	0.681	0.579	0.491
PVX_114330	Plasmodium falciparum CPW-WPC domain containing protein	W43	185	24-185 (162)	WGCF	One-step Ni column (*2*)	0.578	0.633	0.549	0.520
PVX_094830	hypothetical protein, conserved	W06	250	19-end (232)	WGCF	One-step Ni column	0.575	0.689	0.582	0.522
PVX_094350	hypothetical protein, conserved	W41	1220	2-615 (614)	WGCF	One-step Ni column (*2*)	0.573	0.628	0.585	0.498
PVX_092990	tryptophan-rich antigen (Pv-fam-a)	W13	1414	1126-1414 (289)	WGCF	One-step Ni column	0.569	0.692	0.586	0.591
PVX_125738	unspecified product	W38	786	1-786 (786)	WGCF	One-step Ni column	0.567	0.662	0.587	0.581
PVX_121897	tryptophan-rich antigen (Pv-fam-a)	W24	275	24-end (252)	WGCF	One-step Ni column	0.567	0.545	0.571	0.499
PVX_123685	histone-lysine N-methyltransferase, H3 lysine-4 specific (SET10), putative	W37	1963	1320-end (644)	WGCF	One-step Ni column	0.566	0.587	0.637	0.540
PVX_112675	unspecified product	W07	312	33-end (280)	WGCF	One-step Ni column	0.564	0.676	0.615	0.580
PVX_101530	Plasmodium exported protein, unknown function	W09	367	38-end (330)	WGCF	One-step Ni column	0.564	0.651	0.597	0.507
PVX_088820A	tryptophan-rich antigen (Pv-fam-a)	W22	316	58-end (259)	WGCF	One-step Ni column	0.559	0.691	0.589	0.529
PVX_082650	merozoite surface protein 7 (MSP7), putative	W19	453	24-end (429)	WGCF	One-step Ni column	0.558	0.573	0.503	0.479
PVX_097680	merozoite surface protein 3 (MSP3.3)	W28	1016	21-end (996)	WGCF	One-step Ni column	0.556	0.717	0.721	0.632
PVX_080665	hypothetical protein, conserved	W45	553	25-553 (529)	WGCF	One-step Ni column (*2*)	0.553	0.661	0.572	0.487
PVX_088910	GPI-anchored micronemal antigen, putative (GAMA)	W54	771	22-551 (530)	*E. coli*	Two-step affinity (*3*)	0.552	0.639	0.537	0.495

PVX_098915	subpellicular microtubule protein 1 (SPM1), putative	W21	521	1-521 (521)	WGCF	One-step Ni column	0.542	0.652	0.628	0.613
PVX_101590	reticulocyte-binding protein 2 (RBP2), like (RBP2-P2)	W52	641	161-641 (481)	*E. coli*	2x affinity + size exclusion (*5*)	0.538	0.634	0.601	0.584
PVX_088860	sporozoite invasion-associated protein 2 (SIAP2), putative	W03	412	33-end (380)	WGCF	One-step Ni column	0.526	0.706	0.611	0.609
PVX_090330	reticulocyte binding protein 2 precursor (PvRBP-2), putative	W36	623	31-141 (111)	WGCF	One-step Ni column	0.516	0.622	0.526	0.500
PVX_090240	cysteine-rich protective antigen, putative (CyRPA)	W56	366	27-366 (340)	Baculovirus	1x affinity + size exclusion (*5*)	0.496	0.747	0.538	0.606
PVX_117880	rhoptry neck protein 2 (RON2), putative	W23	2203	21-198 (178)	WGCF	One-step Ni column	0.475	0.633	0.573	0.565
PVX_125728	unspecified product	W25	279	30-end (250)	WGCF	One-step Ni column	0.443	0.576	0.538	0.491

[a]PlasmoDB release 36 (http://plasmodb.org/plasmo/), [b]GenBank

References

1. J. Hietanen, A. Chim-Ong, T. Chiramanewong, J. Gruszczyk, W. Roobsoong, W. H. Tham, J. Sattabongkot, W. Nguitragool, Gene Models, Expression Repertoire, and Immune Response of Plasmodium vivax Reticulocyte Binding Proteins. *Infect Immun* **84**, 677-685 (2015).
2. F. Lu, J. Li, B. Wang, Y. Cheng, D. H. Kong, L. Cui, K. S. Ha, J. Sattabongkot, T. Tsuboi, E. T. Han, Profiling the humoral immune responses to Plasmodium vivax infection and identification of candidate immunogenic rhoptry-associated membrane antigen (RAMA). *J Proteomics* **102**, 66-82 (2014).
3. J. Healer, J. K. Thompson, D. T. Riglar, D. W. Wilson, Y. H. Chiu, K. Miura, L. Chen, A. N. Hodder, C. A. Long, D. S. Hansen, J. Baum, A. F. Cowman, Vaccination with conserved regions of erythrocyte-binding antigens induces neutralizing antibodies against multiple strains of Plasmodium falciparum. *PLoS One* **8**, e72504 (2013).
4. J. L. Cole-Tobian, P. Michon, M. Biasor, J. S. Richards, J. G. Beeson, I. Mueller, C. L. King, Strain-specific duffy binding protein antibodies correlate with protection against infection with homologous compared to heterologous plasmodium vivax strains in Papua New Guinean children. *Infect Immun* **77**, 4009-4017 (2009).
5. C. T. Franca, M. T. White, W. Q. He, J. B. Hostetler, J. Brewster, G. Frato, I. Malhotra, J. Gruszczyk, C. Huon, E. Lin, B. Kiniboro, A. Yadava, P. Siba, M. R. Galinski, J. Healer, C. Chitnis, A. F. Cowman, E. Takashima, T. Tsuboi, W. H. Tham, R. M. Fairhurst, J. C. Rayner, C. L. King, I. Mueller, Identification of highly-protective combinations of Plasmodium vivax recombinant proteins for vaccine development. *Elife* **6**, (2017).

Table S3: Association of antibody level with current *P. vivax* infection. Logistic regression model, adjusted for age and sex, and occupation for Thailand and Brazil. P values were calculated using the logistic regression function in STATA.

	Thailand					Brazil					Solomon Islands				
Protein	Odds Ratio	95% CI - lower	95% CI - upper	P value	n	Odds Ratio	95% CI - lower	95% CI - upper	P value	n	Odds Ratio	95% CI - lower	95% CI - upper	P value	n
PVX_090265	7.70	3.59	16.54	p<0·0001	826	4.58	2.69	7.80	p<0.0001	925	3.66	2.20	6.11	p<0·0001	751
PVX_090240	6.76	2.52	18.17	p<0·0001	826	1.68	1.10	2.56	0.016	925	2.35	1.43	3.84	0.001	751
PVX_094255A	6.13	3.00	12.54	p<0·0001	829	6.47	3.67	11.41	p<0.0001	925	3.94	2.60	5.98	p<0·0001	751
PVX_099930B	6.08	2.35	15.69	p<0·0001	826	1.91	1.15	3.16	0.012	925	0.76	0.43	1.35	0.349	751
PVX_090325	6.04	2.77	13.15	p<0·0001	826	4.36	2.72	6.99	p<0.0001	925	1.31	0.75	2.30	0.347	751
PVX_094255B	6.01	2.80	12.89	p<0·0001	826	6.49	3.93	10.73	p<0.0001	925	6.30	4.21	9.44	p<0·0001	751
PVX_092995	5.57	2.22	14.00	p<0·0001	826	3.23	2.04	5.11	p<0.0001	925	1.35	0.86	2.11	0.19	751
PVX_097715	5.27	2.32	11.96	p<0·0001	829	2.20	1.23	3.95	0.008	925	1.37	0.85	2.21	0.191	751
PVX_084720	5.10	2.54	10.23	p<0·0001	829	1.85	1.24	2.76	0.003	925	0.94	0.52	1.70	0.839	751
PVX_097625	4.80	2.44	9.43	p<0·0001	826	2.65	1.79	3.92	p<0.0001	925	3.19	2.02	5.04	p<0·0001	751
PVX_097720	4.75	2.69	8.37	p<0·0001	826	4.10	2.54	6.61	p<0.0001	925	4.66	2.93	7.41	p<0·0001	751
PVX_121920	4.55	2.68	7.73	p<0·0001	826	3.85	2.19	6.75	p<0.0001	925	2.79	1.59	4.91	p<0·0001	751
PVX_091710	4.50	2.26	8.95	p<0·0001	829	2.38	1.53	3.72	p<0.0001	925	0.83	0.46	1.49	0.525	751
PVX_090970	4.44	1.78	11.06	0.001	829	2.50	1.52	4.11	p<0.0001	925	1.55	0.96	2.51	0.072	751
PVX_090330	4.41	2.41	8.07	p<0·0001	826	2.34	1.63	3.34	p<0.0001	925	1.92	1.13	3.24	0.015	751
KMZ83376.1	4.39	2.10	9.19	p<0·0001	826	4.34	2.72	6.92	p<0.0001	925	3.14	1.89	5.22	p<0·0001	751
PVX_084340	4.26	2.09	8.70	p<0·0001	826	2.33	1.41	3.88	0.001	925	1.68	0.95	3.00	0.077	751
PVX_121897	4.18	1.85	9.45	0.001	829	2.28	1.31	3.97	0.004	925	1.25	0.66	2.35	0.497	751
PVX_099980	4.13	2.18	7.84	p<0·0001	829	1.75	1.05	2.91	0.031	925	2.96	2.23	3.94	p<0·0001	751
PVX_000930	4.11	2.26	7.48	p<0·0001	826	2.88	1.98	4.21	p<0.0001	925	2.33	1.57	3.46	p<0·0001	751
PVX_096995	4.02	2.24	7.20	p<0·0001	829	2.99	1.96	4.57	p<0.0001	925	3.69	2.48	5.51	p<0·0001	751
PVX_101530	3.89	2.13	7.10	p<0·0001	829	1.89	1.23	2.89	0.004	925	1.20	0.71	2.04	0.504	751
PVX_087885A	3.79	2.01	7.14	p<0·0001	829	2.66	1.75	4.03	p<0.0001	925	2.99	2.00	4.49	p<0·0001	751
PVX_099930A	3.79	1.72	8.34	0.001	826	3.20	1.98	5.16	p<0.0001	925	1.30	0.76	2.23	0.342	751

PVX_095055	3.78	2.14	6.66	p<0·0001	826	2.89	1.96	4.24	p<0.0001	925	2.64	1.86	3.75	p<0·0001	751
PVX_097680	3.74	2.23	6.25	p<0·0001	826	3.00	1.82	4.94	p<0.0001	925	1.91	1.35	2.71	p<0·0001	751
PVX_123685	3.71	1.79	7.71	p<0·0001	826	2.15	1.42	3.24	p<0.0001	925	1.41	0.90	2.19	0.13	751
PVX_101590	3.62	1.95	6.72	p<0·0001	826	2.23	1.41	3.53	0.001	925	1.99	1.21	3.26	0.007	751
PVX_087885B	3.61	1.84	7.11	p<0·0001	826	2.22	1.41	3.50	0.001	925	2.00	1.27	3.16	0.003	751
PVX_088860	3.59	1.78	7.26	p<0·0001	829	1.34	0.85	2.10	0.210	925	1.08	0.61	1.95	0.784	751
PVX_117385	3.57	1.96	6.50	p<0·0001	829	2.08	1.29	3.38	0.003	925	1.26	0.80	2.00	0.321	751
PVX_114330	3.53	1.87	6.67	p<0·0001	826	1.93	1.16	3.23	0.012	925	1.06	0.64	1.73	0.833	751
PVX_088910	3.53	1.52	8.18	0.003	826	3.27	1.83	5.86	p<0.0001	925	2.53	1.42	4.51	0.002	751
PVX_082700	3.51	1.76	6.99	p<0·0001	826	2.76	1.67	4.58	p<0.0001	925	2.40	1.48	3.89	p<0·0001	751
PVX_088820A	3.36	1.51	7.51	0.003	829	3.00	1.39	6.49	0.005	925	0.88	0.52	1.48	0.633	751
PVX_094350	3.35	1.23	9.13	0.018	826	4.23	2.48	7.23	p<0.0001	925	0.69	0.40	1.17	0.166	751
PVX_092990	3.32	1.31	8.37	0.011	829	2.70	1.46	5.01	0.002	925	1.26	0.74	2.15	0.392	751
PVX_098915	3.27	1.66	6.41	0.001	829	1.20	0.73	1.98	0.477	925	1.00	0.62	1.64	0.985	751
PVX_082735	3.27	1.61	6.63	0.001	826	2.12	1.41	3.17	p<0.0001	925	2.43	1.62	3.64	p<0·0001	751
PVX_003770	3.26	1.73	6.14	p<0·0001	829	1.96	1.27	3.01	0.002	925	1.67	1.03	2.72	0.039	751
PVX_112670	3.24	1.79	5.86	p<0·0001	829	3.06	1.95	4.81	p<0.0001	925	3.62	2.29	5.73	p<0·0001	751
PVX_088820B	3.16	1.16	8.64	0.025	826	6.71	3.32	13.56	p<0.0001	925	0.90	0.51	1.60	0.724	751
PVX_001000	3.15	1.41	7.01	0.005	826	1.76	1.16	2.67	0.008	925	0.95	0.58	1.56	0.841	751
PVX_112690	3.15	1.73	5.74	p<0·0001	829	2.31	1.49	3.59	p<0.0001	925	0.97	0.56	1.70	0.923	751
PVX_080665	3.10	1.66	5.76	p<0·0001	826	1.57	1.09	2.28	0.016	925	1.03	0.63	1.69	0.905	751
PVX_082670	3.04	1.60	5.80	0.001	826	3.03	1.85	4.98	p<0.0001	925	2.18	1.52	3.10	p<0·0001	751
PVX_094830	2.99	1.56	5.74	0.001	829	1.89	1.23	2.89	0.004	925	1.59	0.97	2.61	0.064	751
PVX_117880	2.96	1.48	5.92	0.002	829	2.28	1.49	3.48	p<0.0001	925	1.33	0.83	2.15	0.24	751
PVX_125728	2.94	1.36	6.38	0.006	829	1.49	1.06	2.10	0.021	925	1.04	0.69	1.57	0.842	751
PVX_112675	2.80	1.49	5.28	0.001	829	1.74	1.21	2.49	0.003	925	1.44	0.80	2.60	0.222	751
PVX_112680	2.80	1.45	5.42	0.002	829	1.97	1.26	3.08	0.003	925	1.00	0.59	1.67	0.992	751
PVX_082645	2.78	1.28	6.07	0.01	826	3.08	1.96	4.82	p<0.0001	925	1.97	1.27	3.06	0.003	751

PVX_125738	2.77	1.41	5.43	0.003	826	3.08	1.97	4.83	p<0.0001	925	1.27	0.72	2.24	0.4	751
PVX_003555	2.73	1.60	4.64	p<0·0001	829	1.58	1.07	2.34	0.021	925	0.82	0.46	1.46	0.511	751
PVX_082650	2.43	1.44	4.08	0.001	829	2.07	1.42	3.02	p<0.0001	925	2.11	1.43	3.12	p<0·0001	751
PVX_098582	2.30	1.11	4.77	0.026	826	2.63	1.56	4.42	p<0.0001	925	1.67	0.89	3.15	0.113	751
PVX_110810B	2.23	1.33	3.73	0.002	826	2.28	1.51	3.44	p<0.0001	925	1.87	1.26	2.78	0.002	751
AAY34130.1	2.11	1.33	3.35	0.002	826	2.29	1.44	3.64	p<0.0001	925	1.79	1.22	2.62	0.003	751
PVX_110810A	2.08	1.33	3.25	0.001	826	2.20	1.37	3.53	0.001	925	1.96	1.35	2.83	p<0·0001	751
PVX_098585	2.07	1.15	3.75	0.016	826	1.53	0.97	2.41	0.068	925	2.28	1.53	3.40	p<0·0001	751

Table S4. Epidemiological overview of data sets used in antigen discovery and validation phases. Individuals in the antigen discovery phase were recruited following a clinical episode of *P. vivax*.

*denotes PCR prevalence in the general population.

Population	**N: number of participants**	**n: subset with antibody measurements**	**age (years)** median (range)	**sex** % female	**PCR *Pv*PR**	**time since last PCR positive sample**			
						current	<9 months	9-12 months	not detected
(A) *Antigen discovery data*									
Thailand	57	32	29 (7, 71)	44%	11.4%*	–	–	–	–
Brazil	91	33	36 (16, 56)	21%	5.0%*	–	–	–	–
(B) *Validation data*									
Thailand	999	829	24 (1, 78)	54.7%	3.33%	25	47	25	732
Brazil	1274	928	25 (0, 103)	50.7%	5.21%	40	165	31	692
Solomon Islands	860	754	5.6 (0.5, 12.7)	51.6%	11.92%	93	172	29	566
Victorian Blood Donor Registry (VBDR)	102	102	39 (18, 68)	69.6%	0.0%	0	0	0	102
Australian Red Cross (ARC)	100	100	52 (18, 77)	54.0%	0.0%	0	0	0	100
Thai Red Cross (TRC)	72	72	–	–	0.0%	0	0	0	72
Rio State Blood Bank (RBB)	96	96	–	–	0.0%	0	0	0	96